THE REPUBLIC OF TURKEY
MUĞLA SITKI KOÇMAN UNIVERSITY
GRADUATE SCHOOL OF NATURAL AND APPLIED SCIENCES

DEPARTMENT OF GEOLOGICAL ENGINEERING

SLUG TESTS: EXPERIMENTAL STUDY OF HYDRAULIC SHOCK TESTS ON THE OISE STRUCTURES (APPLICATION TO THE HYDROGEOLOGICAL EXPERIMENTAL SITE OF BEAUVAIS)

MASTER OF SCIENCE THESIS

CİHAN OKUTAN

NOVEMBER 2021
MUĞLA

C. OKUTAN DEPT. OF GEOLOGICAL ENGINEERING MASTER THESIS MUĞLA 2021

THE REPUBLIC OF TURKEY
MUĞLA SITKI KOÇMAN UNIVERSITY
GRADUATE SCHOOL OF NATURAL AND APPLIED SCIENCES

DEPARTMENT OF GEOLOGICAL ENGINEERING

SLUG TESTS: EXPERIMENTAL STUDY OF HYDRAULIC SHOCK TESTS ON THE OISE STRUCTURES (APPLICATION TO THE HYDROGEOLOGICAL EXPERIMENTAL SITE OF BEAUVAIS)

MASTER OF SCIENCE THESIS

CİHAN OKUTAN

NOVEMBER 2021
MUĞLA

MUĞLA SITKI KOÇMAN ÜNİVERSİTESİ

Graduate School of Natural and Applied Sciences

APPROVAL OF THE THESIS

The thesis submitted by CİHAN OKUTAN with the title of **"SLUG TESTS: EXPERIMENTAL STUDY OF HYDRAULIC SHOCK TESTS ON THE OISE STRUCTURES (APPLICATION TO THE HYDROGEOLOGICAL EXPERIMENTAL SITE OF BEAUVAIS)"** has been unanimously/majority accepted by the jury members to fulfill the requirements for the necessary conditions for master degree of Department of Geological Engineering at 04/11/2021.

THESIS DEFENCE JURY

Dr. Öğr. Günseli ERDEM **(Head of Jury)** Signature:

Department of Civil Engineering,
Nişantaşı University, İstanbul _____

Assoc. Prof. Dr. Bedri KURTULUŞ **(Supervisor)** Signature:

Department of Geological Engineering,
Muğla Sıtkı Koçman University, Muğla _____

Assoc. Prof. Dr. Can CANOĞLU **(Member)** Signature:

Environmental Engineering,
Sinop University, Sinop _____

APPROVAL OF HEAD OF THE DEPARTMENT

Assoc. Prof. Dr. Sena AKÇER-ÖN Signature:

Head of Department, Department of Geological Engineering,
Muğla Sıtkı Koçman University, Muğla _____

Assoc. Prof. Dr. Bedri KURTULUŞ Signature:

Supervisor, Department of Geological Engineering,
Muğla Sıtkı Koçman University, Muğla _____

Date: 04/11/2021

I hereby declare that all information in this document has been obtained and presented in accordance with academic rules and ethical conduct. I also declare that, as required by these rules and conduct, I have fully cited and referenced all material and results that are not original to this work.

Cihan OKUTAN

01/10/2021

ÖZET

SLUG TESTLER: OISE YAPILARINDA HİDROLİK ŞOK TESTLERİNİN DENEYSEL ÇALIŞMASI

(BEAUVAIS HİDROJEOLOJİK DENEY ALANI'NDA UYGULAMALAR)

Cihan OKUTAN

Yüksek Lisans Tezi

Fen Bilimleri Enstitüsü

Jeoloji Mühendisliği Anabilim Dalı

Danışman: Doç. Dr. Bedri KURTULUŞ

İkinci (Ortak) Danışman: Doç. Dr. Lahcen ZOUHRI

Kasım 2021, 49 sayfa

Üst Kretase tebeşir akiferi, Oise bölümündeki (Hauts-de-France) endüstriyel ve tarımsal faaliyetler için hayati bir su kaynağıdır. Akiferin hidrodinamik karakterizasyonunu elde etmek için saha testleri yapılmıştır. Bu çalışmada, maliyet etkinliği, hızlı uygulama ve hızlı yanıt gibi nedenlerle tercih edilen yaygın bir saha test yöntemi olan slug testi ile Beauvais Hidrojeolojik Deney Alanı'nın (HESB, UniLasalle) hidrolik özelliklerinin belirlenmesini amaçlamaktadır. Hidrolik araştırmalardan elde edilen sonuçlar, hidrojeolojik model oluşturulurken ve yeraltı suyu sirkülasyonunu belirlemek için faydalı olan HESB geçirgenlik değerlerinin mekansal dağılımını belirlemek için sayısal kod geliştirilirken kullanılacaktır. Ayrıca, gelecekte kurulması planlanan pompa sistemi için uygun olan hidrojeolojik kuyuları tanımlamak için gereken parametreler hakkında bilgi sağlayacaktır.

Çalışma alanındaki on sekiz adet kuyuda çok sayıda deney yapılmıştır. Yeraltı suyunun davranışını anlamak için uygulanan testlerin analiz edilmesi gerekir. Deneysel sonuçlar, serbest akiferler için geçerli olan Bouwer & Rice yöntemi ile analiz edilmiştir. AQTESOLV adlı bir akifer test analiz yazılımı kullanılarak analitik çözümler gerçekleştirilmiştir. Sahanın deneyimlenen hidrolik iletkenlik değeri 4.43e-8 ile 7.56e-6 m/s arasında değişmektedir. Aynı zamanda, yeraltı suyu şarjı, su tablası dalgalanmaları (WTF) yönteminin epizodik olay tabanlı yaklaşımları ile tahmin edildi. Bu çalışmada kullanılan diğer bir yaklaşım ise, kararlı durum ve geçici durum modellemeleridir. Bu modeller, hidrolik iletkenlik dağılım haritaları ve geçirgenlik değerleri ile sonuçlanmıştır.

Anahtar Kelimeler: Hidrolik İletkenlik, Slug Test, Modelleme, MODFLOW, Tebeşir Akiferi

ABSTRACT

SLUG TESTS: EXPERIMENTAL STUDY OF HYDRAULIC SHOCK TESTS ON THE OISE STRUCTURES

(APPLICATION TO THE HYDROGEOLOGICAL EXPERIMENTAL SITE OF BEAUVAIS)

Cihan OKUTAN

Master of Science (M.Sc.)

Graduate School of Natural and Applied Sciences

Department of Geological Engineering

Supervisor: Assoc. Prof. Dr. Bedri KURTULUŞ

Co-supervisor: Assoc. Prof. Lahcen ZOUHRI

November 2021, 49 pages

The Upper Cretaceous chalk aquifer is a vital water resource for industrial and agricultural activities in the Oise department (Hauts-de-France). To obtain the hydrodynamic characterization of the aquifer, field tests were implemented. This study aims to determine the hydraulic properties of the Hydrogeological Experimental Site of Beauvais (HESB, UniLasalle) with series of slug tests, which is a common field test method preferred for reasons such as cost-effectiveness, fast implementation, and quick response. Results obtained from the hydraulic investigations will be used while creating the hydrogeological model and developing the numerical code to identify the spatial distribution of the HESB transmissivity values which is useful to determine the groundwater circulation and potential mitigation of groundwater pollution. It will also provide information about the parameters required to define hydrogeological wells that are favorable for installing the pump system.

Numerous experiments were carried out in eighteen wells in the study area. For understanding the behavior of groundwater, the applied tests need to be analyzed. Experimental results were analyzed with the Bouwer & Rice method, which is applicable for unconfined aquifers. Analytical solutions were performed by using an aquifer test analysis software called AQTESOLV. Experienced hydraulic conductivity value of site varies between 4.43e-8 and 7.56e-6 m/s. Concurrently, the groundwater recharge was estimated with episodic event-based approaches of the water table fluctuations (WTF) method. Another approach used in this study is the steady-state and transient-state modeling. These models resulted in hydraulic conductivity distribution maps and transmissivity values.

Keywords: Hydraulic Conductivity, Slug Test, Modelization, MODFLOW, Chalk Aquifer

To my wife,
Who always encourages me with her love and unconditional support.

ACKNOWLEDGMENT

I would first like to thank my supervisor, Assoc. Prof. Bedri KURTULUŞ and co-supervisor, Assoc. Prof. Lahcen ZOUHRI, for providing guidance and feedback throughout this study.

I am also grateful to Sıtkı Koçman Foundation and French Embassy Turkey for providing me scholarship funding.

And my biggest thanks to my wife Hande OKUTAN, my dear parents, brother, and sister for their constant supports through my life.

TABLE OF CONTENTS

LIST OF TABLES

LIST OF FIGURES

SYMBOLS AND ABBREVIATIONS

°C	Degree celcius
µS/cm	Microsiemens per second
WTF	Water table fluctuation
MRC	Master recession curve
EMR	Episodic master recession
PEST	Parameter estimation
RMS	Root mean square

1. INTRODUCTION

To understand the behavior of groundwater and pollution, critical parameters are needed. Two of these are permeability and hydraulic conductivity. For determining these properties of the environment, hydrogeological field tests need to be implemented. With slug tests, hydrodynamic parameters include hydraulic conductivity, transmissivity, and storativity can be determined (Alfaifi, 2015; Black, 1978; Ola et al., 2016).

Slug test is a widely preferred in-situ investigation method due to its fast implementation, quick response, and cheapness (Fabbri et al., 2012). The rate of water level equilibrium has a relation with the horizontal hydraulic conductivity of the local test area. This method consists of an agent's instantaneous changing in water level and measuring the water level's recovery after the change (Butler, 2019; Fetter, 2000; Zlotnik & McGuire, 1997). This agent can be a solid material whose volume is known or volume of water injected into (or removed from) the well. After the change of water level, the hydraulic conductivity of formation can be determined with the recovery data obtained from well and theoretical models(Butler, 1996). It also has many advantages that some of them are written above; it is an inexpensive test. While application of slug test, complex equipment, and human resources are not needed. Also, it is a quick test to take responses (data). It can be helpful in formations that have low hydraulic conductivity. In addition, as in the study mentioned by Ola et al. (2016), it would be a useful method in contaminated areas when the slug test is implemented without extracting water. This provides no contact to the contamination in groundwater, consequently, not needed to treat the contaminated water, as in the pumping test. The cost of remediation of the contaminated water extracted from the well is absent in a slug test operation.

The slug test can be a valuable way of determining the hydraulic conductivity in both confined and unconfined aquifers. There are several methods for calculating the

hydraulic conductivity depend on aquifer type, presence of well skins, underdamped – overdamped conditions, multi-well tests, and position of water table relative to the well screen.

The slug tests may provide the spatial variability of contamination. That can be expressed as; vertical and horizontal hydraulic conductivity measurements can be made in the investigated area with a series of slug tests in the wells (Butler, 2019). On the other hand, according to Kruseman and de Ridder (1990), the slug tests are only useful for calculating the characteristics of a small environment near well; compare with pumping tests. Otherwise, Audouin et al. (2008) performed some slug tests in the experimental site of Poitiers (France) with a distance between observation wells and test wells are 50 to 140 m and states that the slug test can be used in studies in karstic and fractured hydrogeological areas together with pumping tests.

The slug test is also called the rising head or falling head test. When the water is lowered rapidly and measuring while rising water, it is called as “rising head” and vice versa. Also, it has terminology about the response of the aquifer. If an aquifer has low hydraulic conductivity, it gives an overdamped response. The graph of normalized head data vs. time is like a straight line; if the aquifer has high hydraulic conductivity, it provides an underdamped response with oscillations (Fetter, 2000).

The main objective of this study is to estimate the hydrodynamic characteristic of the Hydrogeological Experimental Site of Beauvais (HESB, Unilasalle) by performing a series of slug test experiments and developing a numerical groundwater flow model to characterize the aquifer properties.

1.1. Study Area

The Experimental Site of Beauvais (Polytechnic Institute Unilasalle) is in the Oise department of the Hauts-de-France region, north of France, as shown in Figure 1.1. The study area includes 20 hydrogeological drillings with the depth of 110 m. There are two sets of wells which has different diameters, 125 mm and 160 mm. All wells are cased partly screened PVC after 30 m non-screened part. In natural conditions, the water level in the experimental site ranges between 37 and 42 m below the ground

surface. Since there is an inactive pump system installed in F-2, one of the wells in the experimental site, it is not included in the data sets in this study.

The study area is located on the Paris sedimentary basin and consists of Cenomanian units that lie on the Albian basement (Zouhri & Lutz, 2010). The aquifer beneath the experimental site is accepted as unconfined (Zghibi et al., 2016). The formations in the study area are defined by Tirat et al. (1969) as seen following Lower Albian is represented by green sand (glauconitic sands) that include coarse-sized sands; gray-green to red-colored; includes lignite, pyrite, and glauconite. The thickness of the formation is about 20 to 30 m. Upper Albian is represented by Gault clays that are a mixing of clayey, sandy, and glauconitic layers (Knight, 1999). Upper Albian is observed to be 50 to 60 m thick in the southeast of Beauvais. The thickness of Cenomanian is about 60 m includes siliceous clay detrital formations (Gille et al., 2002). Nodular calcareous siliceous units called gaize lying below sandy clays and white to green colored chalk without chert or with gray chert, which is altered glauconious and clayey represent Cenomanian units (Tirat et al., 1969).

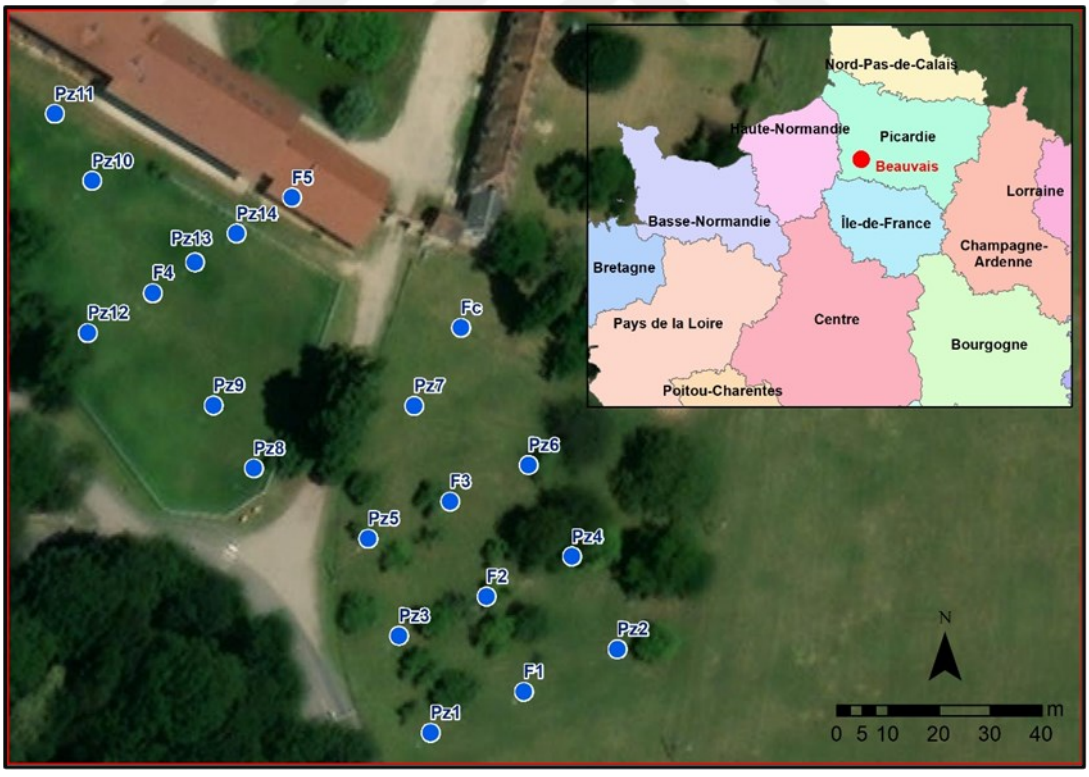

Figure 1.1. Location map of the study area (Beauvais, Unilasalle)

Turonian is represented by marly chalk or gray marl with chert. Senonian units with a maximum thickness of 70 meters that are white to yellow or gray chalk with chert. Quaternary deposits are observed in the upper parts of the stratigraphy.

The main groundwater flow of the Cenomanian chalk aquifer is defined as towards the Le Thérain River (Zouhri & Lutz, 2010). Le Thérain, which is a tributary of the Oise River, is formed along the anticline of Pays de Bray and flows along the syncline in Senonian units (Harb & Roussel, 1987).

1.1.1. Chalk aquifer

The groundwater of the Cretaceous chalk aquifer is a significant resource for a large part of NW Europe, contains northern France, south of England, some parts of Belgium, Germany, the Netherlands, and Denmark (Lapworth et al., 2015). The chalk outcrops are seen in an area of 70 000 km2 around the Paris basin (Crampon et al., 1993). Approximately 12 billion m3/annual water is supplied from the chalk aquifer, which covers 20 % of French territory, about 110 000 km² (Lallahem, 2002). It is also extracted for various purposes such as construction, agricultural purposes, cement industry, paint, and paper industry (Crampon et al., 1993).

The hydrogeological characteristic of chalk varies from one region to another with identifiable properties such as geomorphological settings, the depth of the aquifer, and geology. The capacity of water storage and transmissivity in the chalk aquifer is related to sandy clayey compositions, weathering, joint-fracture systems developed due to tectonism, and karstification that develops accordingly (Crampon et al., 1993). There are many studies about double porosity and double permeability of chalk (Baran et al., 2008; Barhoum et al., 2014; Brouyère, 2006; Cao et al., 2020; Chen et al., 2019; Crampon et al., 1993, 1996; Ireson et al., 2006; Lallahem, 2002). The rock matrix has low permeability, but fissures and karstic intersections provide high permeability, although low porosity (Crampon et al., 1993). Crampon et al. (1996) defined the Cretaceous Chalk as limestone with 30% to 40% porosity and high permeability due to interrelated fractures; the specific yield is lower than 2%. Allen et al. (1997) and Zouhri and Lutz (2016) emphasize that chalk differs significantly in different regions and stratigraphy. The porosity of chalk varies over a wide range. According to the

porosity measurements made on more than two thousand chalk samples taken from 75 points in England, the mean porosity varies between 22.9 and 38.8 % (Bloomfield et al., 1995).

In the studies carried out in the Geovexin Project (LPG underground storage project), it has been observed that the chalk has a very low hydraulic conductivity (Defossez et al., 2013). Crampon et al. (1993) states that deeper levels of Turonian chalk (around 150 m) have lower than 1e-7 m/s and hydraulic conductivity of Santonian chalk (75 m deep) varies between 1.5e-7 m/s and 3.2e-8 m/s. Also, it shows a value of around 2.5e-6 m/s inside the fissured chalk. The hydraulic conductivity around Tours (France) varies between 1e-6 m/s and 1e-4 m/s, and around Sénonais, it is 4e-3 m/s (Crampon et al., 1993).

The chalk aquifer in the department of Oise has double porosity of joints and pores. The hydraulic conductivity related to interstices is generally lower than 1e-5 m/s despite a significant total porosity (more than 30%). On the other hand, the joint fracture system in the aquifer provides higher hydraulic conductivity (between 1e-3 m/s and 1e-2 m/s) (Bault et al., 2012). In other regions close to the study area, hydraulic conductivity values close to these values were obtained; 3e-4 m/s at Ons-en-Bray and 3.8e-3 m/s at Lacroix-Sait-Ouen (Zouhri & Armand, 2019).

In the study area, the heterogeneous character of hydraulic conductivity due to fractures generates anisotropic distribution in the horizontal and vertical directions. According to Domenico and Schwartz (1998), the chalk's horizontal and vertical conductivities vary between 1e-10 m/s to 1e-8 m/s and 5e-11 m/s to 5e-9 m/s, respectively. (Lutz and Zouhri (2015) mentioned that the vertical conductivity of the study area differs between 2e-5 m/s and 2e-2 m/s (Zouhri & Lutz, 2016).

1.1.2. Water quality

Studies conducted in 19 wells in the experimental site are useful in protecting and managing water resources due to increased industrial and agricultural activities. In particular, water demand in irrigation in agricultural activities covering large areas in the department, in industrial areas, and drinking water in urban areas are provided from the chalk aquifer. Although there has been a decrease in economic activities in recent

years, excessive pumping in densely populated and industrialized areas dramatically affects the groundwater level in the chalk (Crampon et al., 1993). Zouhri and Armand (2019), stated that inorganic fertilizers consist of nitrogen, potassium, ammonium nitrate, phosphorus, and nitrogen compounds used in agricultural activities that affect groundwater quality. The unconfined parts of the chalk aquifer that underlies on urban areas are the most affected by possible pollution.

As a result of 1-week measurements made within the scope of this study with the multi-sensor probe (Hanna Instruments, n.d.) on F-5, the temperature range is 11-12 °C, mostly 11.5 °C; the pH is around 6.75-7.5, and the electrical conductivity is in the range 600-700 µS/cm.

1.1.3. Climate meteorology

The area covering the experimental site is described as oceanic climate. In winter, dry-cold and humid-warmer climates are seen alternately. The weather is humid and temperate in the summer months due to the aquatic effect (Bault et al., 2012). Measurements of temperature from 1990 to 2020 from MétéoFrance Beauvais meteorological station show that the average minimum temperature is about 4°C and the highest average temperature is about 18 °C as seen on Figure 1.2. January and July are the coldest and warmest months, respectively.

The annual cumulative precipitation between 1990 and 2020 averaged 652.46 mm y^{-1} in Beauvais (

Figure 1.3). Table 1.1 shows the precipitation data of Beauvais. The number of days per year with precipitation greater than 1 mm is 114 on averages of 1990 to 2020. Considering the low average in July and August and the consecutive rainy days in the winter months, the average rainy day per year is almost one day in three days.

Number of days with precipitation (> 1 mm)	Annual per year	114
	Lowest Total Annual	83 (1996)
	Highest Total Annual	154 (2000)
Precipitation height (mm)	Annual per year	652.46
	Lowest Annual Cumulative	416.00 (2005)
	Highest Annual Cumulative	970.40 (2000)

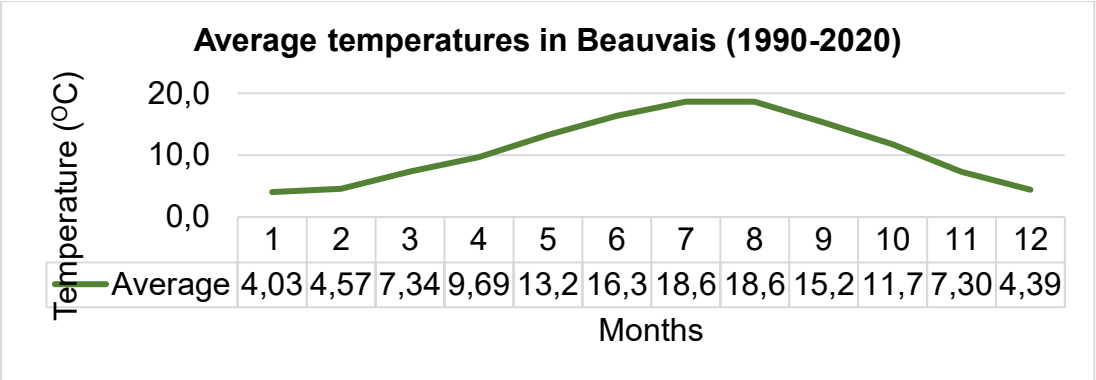

Figure 1.2. Monthly average temperatures in Beauvais (1990-2020)

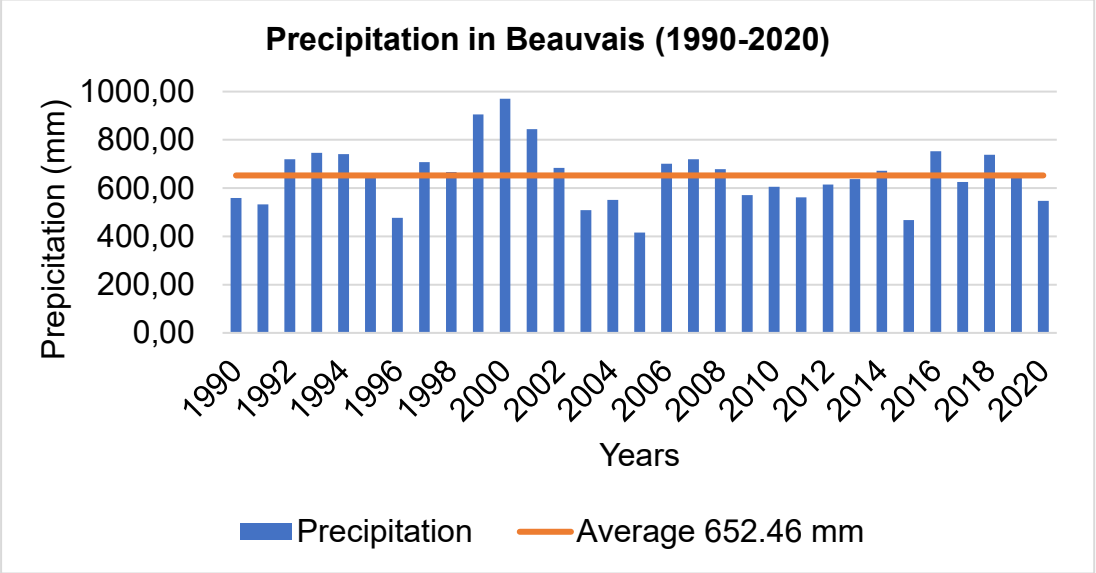

Figure 1.3. Precipitation chart for 1990-2020 MétéoFrance Beauvais station

Table 1.1. Precipitation data of Beauvais

Number of days with precipitation (> 1 mm)	Annual per year	114
	Lowest Total Annual	83 (1996)
	Highest Total Annual	154 (2000)
Precipitation height (mm)	Annual per year	652.46
	Lowest Annual Cumulative	416.00 (2005)
	Highest Annual Cumulative	970.41 (2000)

2. MATERIAL AND METHODS

2.1. Slug Tests

2.1.1. Slug test equipment

There are several pieces of equipment for measuring the parameters, such as depth and pressure. Chalked steel tape, plopper, electric tape, and float-gauge recorder can be used for depth measurements. For pressure measurements, pressure transducers are used. These are for converting the physical measurement to electrical signals (Butler, 2019). The rapid movements of water can be measured with transducers. A barometric sensor is also required for measuring the changes in air pressure. Also, packer systems can be used for slug tests (Bouwer & Rice, 1976).

In this study, since the slug test was carried out by adding water, the water tank, a water level meter (Solinst Model 107), pressure transducers (VanEssen Instruments, 2021) were used.

2.1.2. Techniques

Slug tests can be implemented with different kinds of methods. The main idea is to change the static water level instantaneously and determine the equilibrium of the water (Alfaifi, 2015). Using a solid slug is the most common method. It is performed with a solid object which is quickly submerged or removed into/from the water level (Butler, 2019). Another method is adding or removing water rapidly. This method can be applied in two ways, pouring the water rapidly into the well or pumping it out from the well quickly. In this study, the rapid water addition method was used. Each technique includes the measurement of the response given from the aquifer. The other method described by Greene and Shapiro (1995) is air pressured (pneumatic) systems. Lastly, with packer systems the static water level in the well can be changed by an

inflatable or mechanical packer; after deflation, the head recovery is measured (Butler, 2019).

2.1.3. Experimental procedure

This procedure was implemented for all tests. The explanations in this section describe what was done in a single well test. Before starting the experiment, the static water level in the well was measured with a water level meter for comparison with the value after the test. The pressure transducer was connected to the computer for defining test information, includes well name, starting time, measuring frequency, etc. The measurement frequency of transducers was selected as per minute, 30 seconds, per 2 seconds, and seconds. In tests that are thought to take a long time due to low conductivity values, most tests were performed with 2 seconds of frequency measurement in order to obtain test data with sufficient resolution.

After, the transducer was placed into the well, as expected, below the groundwater level (submerged). The device was kept stable throughout the measurement. After the transducer started to take measurements, a minimum of 500 liters of water was injected instantaneously. The transducer left until the water level in the test well reached the equilibrium which was determined by the water level meter. After, the transducer was extracted from the well, and the data was downloaded to the computer. Meanwhile, a barometric diver was installed in the site to compensate of atmospheric pressure on the diver in the well. The compensation and calculation of water level measured throughout the test were calculated by the software (VanEssen Instruments, 2021). All tests had been performed after the static water level had been reached.

Minimum three tests were implemented for each well except PZ-11. It has been observed that PZ-11 is not suitable for testing.

2.1.4. Slug test analyzing methods for unconfined aquifers

There are many methods to estimate the hydraulic conductivity values by fitting model procedures that have been studied for about 70 years. Several analytical modeling methods have been developed for different boundary conditions such as confined or

unconfined aquifers, high or low conductivity areas, etc. In this study, the Bouwer & Rice (1976) was used.

2.1.4.1. Bouwer & Rice Method

Bouwer & Rice (1976) derived the solution of rising water level with a sudden extraction of a slug. The Thiem equation was modified as:

$$Q=2\pi KL\ \frac{H_0}{\ln(\frac{R_e}{r_w})} \qquad (2.1)$$

Where;

Q: Flux (L^3/T)

K: Hydraulic conductivity ($L.T^{-1}$)

L: Length of the well screen (L)

H_0: Initial head difference (initial displacement) (L)

R_e: effective radial distance (where the change of water level occurs) (L)

r_w: radius of well (L)

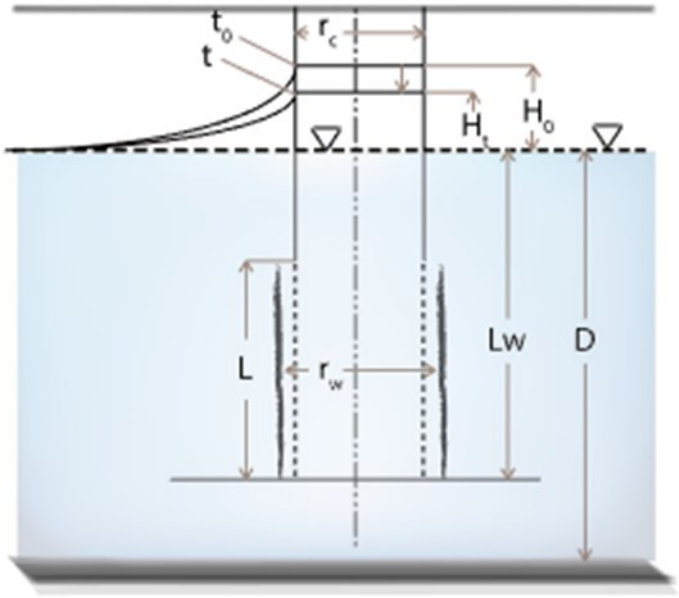

Figure 2.1. Slug test illustration in unconfined aquifer with symbols (Modified from Waterloo Hydrogeologic (2021))

The rate of change (dH/dt) is described with the equation shown below:

$$\frac{dH}{dt} = -\frac{Q}{\pi r_c^2} \tag{2.2}$$

Where πr_c^2 represents the cross-sectional area of the well. So, with equation 2.1 and equation 2.2, Bouwer and Rice (1976) exhibit the equation:

$$K = \frac{r_c^2 \ln(R_e/R_w)}{2L} \frac{1}{t} \ln \frac{H_0}{H_t} \tag{2.3}$$

Where;

H(t): Water drawdown in the well (L)

r_c: radius of the casing (L)

The physical quantities represented by the abbreviations can be seen in Figure 2.1. Also, transmissibility is calculated by equation 2.3 multiply by the saturated aquifer thickness (D).

Re depends on the flow geometry, and it is obtained by length of the well screen, the radius of the well, saturated aquifer thickness. In the same study of Bouwer and Rice (1976), the term of R_e / R_w is calculated with the equation shown below:

$$\ln \frac{R_e}{r_w} = \left[\frac{1.1}{\ln(L_w/r_w)} + \frac{A + B \ln\left[\frac{D-L_w}{r_w}\right]}{\frac{L}{r_w}} \right]^{-1} \tag{2.4}$$

If the length from the water table to the bottom of the well is lower than the saturated aquifer thickness (Lw<D), equation 2.4 should be used. Otherwise, if Lw=D, equation 2.5 should be used. Furthermore, the parameters of A, B, C coefficients are determined with Figure 2.2.

$$\ln\left(\frac{R_e}{r_w}\right) = \left[\frac{1.1}{\ln\left(\frac{L_w}{r_w}\right)} + \frac{C}{\frac{L}{r_w}} \right]^{-1} \tag{2.5}$$

This method has some assumptions; the aquifer is assumed as homogeneous and isotropic. Drawdown around the well is neglected. Head losses as water enter the well are neglected. Also, flow in unsaturated area capillary fringe is neglected.

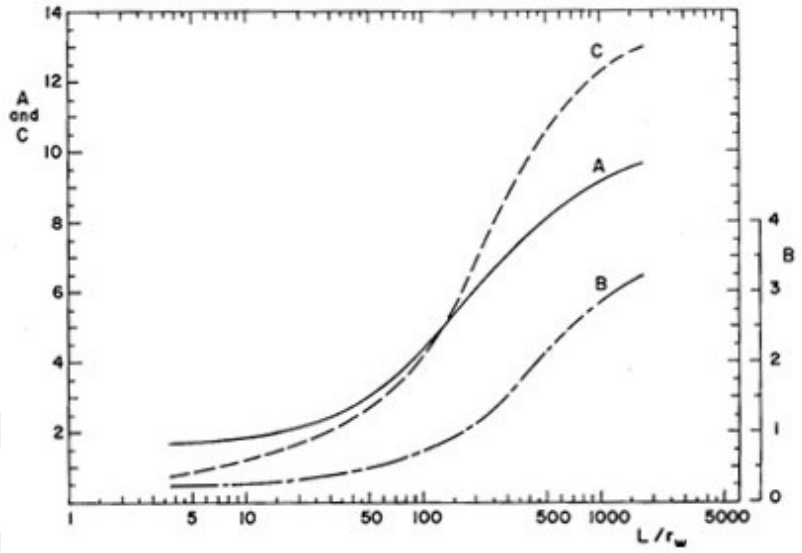

Figure 2.2. Dimensionless A, B, and C parameters (Bouwer & Rice, 1976)

2.1.4.2. Dagan Method

Dagan (1978) submitted a method for calculating the hydraulic conductivity in wells whose screens are across the groundwater level. The only difference from Bouwer and Rice (1976) method is that the Dagan Method accepts no constant head boundary at a distance from the well. The steps of calculation are described as follows (Butler, 2019);

The normalized response data is placed on the graph consist of the logarithmic y-axis and arithmetic x-axis since the start of the experiment, and the fitting line on points is drawn. The slope of the line is calculated.

The line is extended until it intersects the y-axis, and the value on the y-axis is multiplied by 0.368, and the new value is obtained. The new time value (T_0) is also determined from the graph.

Estimation of the parameter Ψ is made for the particular well configuration.

$$\Psi = \frac{\sqrt{K_z / K_r}}{L_e / r_w} \tag{2.6}$$

Where K_z/K_r is the ratio of anisotropy (=1, most cases) (Todd & Mays, 2004)

The P-value, dimensionless flow parameter, is selected from Table 2.1 or Table 2.2 with the Ψ.

Table 2.1. Dimensionless P values for L/D≤0.05 (Butler, 2019)

	L_w / L				
ψ	8	4	2	1.5	1.05
0.2	0.646	0.663	0.705	0.756	1.045
0.1	0.477	0.487	0.505	0.531	0.687
0.067	0.409	0.416	0.429	0.446	0.562
0.05	0.367	0.373	0.385	0.397	0.491
0.033	0.322	0.325	0.335	0.352	0.414
0.025	0.294	0.297	0.305	0.322	0.37
0.02	0.276	0.278	0.287	0.301	0.342
0.013	0.247	0.249	0.255	0.269	0.3
0.01	0.23	0.231	0.238	0.25	0.276
0.0067	0.211	0.21	0.213	0.227	0.248
0.005	0.198	0.199	0.201	0.213	0.23

Table 2.2 Dimensionless P values for Lw=D (Butler, 2019)

	L / D					
ψ	1	0.83	0.67	0.5	0.2	0.1
0.2	1.289	0.723	0.631	0.576	0.51	0.492
0.1	0.8	0.51	0.46	0.428	0.39	0.38
0.05	0.536	0.384	0.354	0.335	0.312	0.306
0.025	0.388	0.305	0.286	0.273	0.258	0.254
0.01	0.279	0.238	0.227	0.219	0.209	0.206

Horizontal hydraulic conductivity has estimated the equation seen below:

$$K_r = \frac{r_c^2 (\frac{1}{P})}{2LT_0} \qquad (2.7)$$

Butler (2019) mentioned that the slug tests are differed by the static water level based on the well screen. In case of the screen of the well which the test is applied on is below the water table causes a slight anomaly, and the model can be created with a linear mathematical model (Figure 2.3.a). On the other hand, if the well screen is across

the water table, it can be represented by nonlinear mathematical equations (Figure 2.3.b).

In the cases where the water table is below the top of the well screen, the drainage of the artificial filter pack is the main parameter that controls the formation response. When the test is applied (initiation has occurred), firstly, the filter pack drains due to high permeability. According to Butler (2019), the water level in the well rises until it is equalized with the water level in the filter pack and then rises together. This behavior causes a double curved line in a logarithmic normalized head graph (Bouwer, 1989).

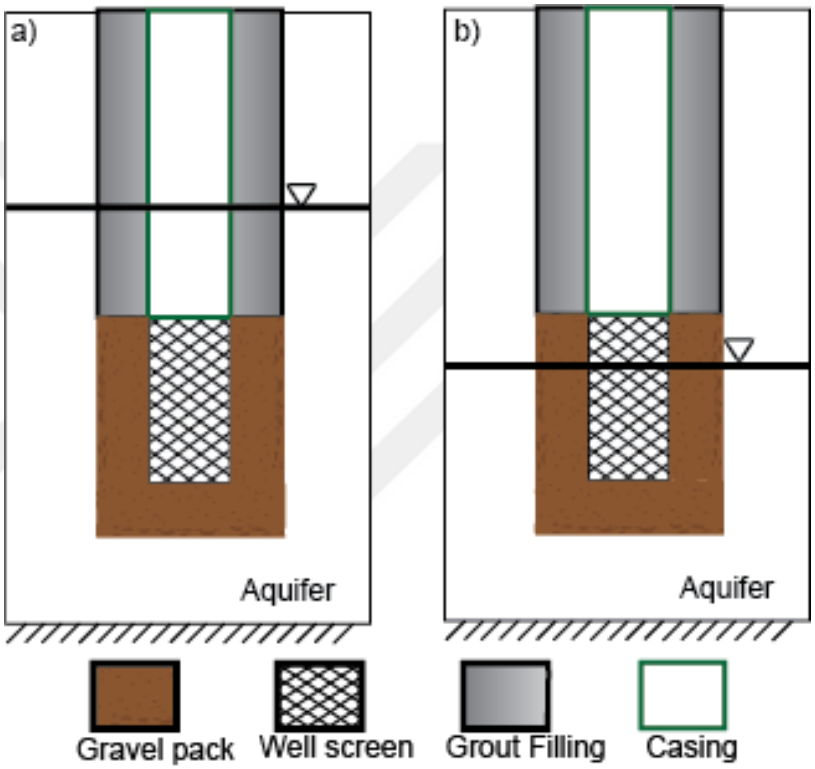

Figure 2.3. Well screen below (left) and above (right) the groundwater level (Modified from Butler (2019))

2.1.5. Analytical solution

The slug tests presented in this study were analyzed with AQTESOLV Pro v4.5, which includes 18 different methods for different conditions of aquifers (Duffield, 2007). Bouwer and Rice (1976) method in the software was used for estimating the hydraulic conductivity from slug test data by curve matching method while using the software. The software has two different curve matching options: automatically and manually.

The automatic curve matching option performs the nonlinear least-squares method to fit the observed and calculated (solution) data by using iterations to minimize the sum of squared residuals. The other option is named visual curve matching procures to the user to fit the curves manually (Duffield, 2007). In the analytical results, the automatic curve matching option was used, and visual curve matching was applied for maximizing the accuracy of fitting within the normalized head ranges recommended by Butler (1996); which is 0.20-0.30 for the best results of the Bouwer and Rice (1976) method.

The input data for AQTESOLV is classified as (1) well geometry, (2) aquifer information, (3) testing range, and (4) observations. The ratio of vertical hydraulic conductivity to horizontal hydraulic conductivity, Kv/Kh, was assumed as 1; it is recommended that the Bouwer and Rice (1976) method should be used for isotropic cases (Alfaifi 2015). As stated by Duffield (2007), in the absence of field-specific information, the aquifer thickness can be estimated; ergo, the aquifer thickness was estimated as 100 m. The other important point while inputting the data to software is the observation part. The data extracted from the pressure transducer is the measurement of water level changes in time. The observation screen of software needs the displacement of the water level. In this regard, the difference between the static water level before the test initiation and the highest water level (initial displacement) after injection was accepted as the highest displacement as well as the beginning of the drawdown. The ratio of subsequent displacement reading to initial displacement refers to the normalized head, which is the y-axis on the resulting graph. The data was entered until the normalized head was 0.05 (Duffield, 2021).

2.2. Calculation of Aquifer Recharge

One of the essential parameters in contaminant transport and flow modeling is the rate of groundwater recharge (Doble & Crosbie, 2017; Healy & Scanlon, 2010). Recharge and discharge are the two significant factors for a groundwater flow model. There are several methods for estimating recharge; these vary depending on the location of the investigated site relative to the groundwater table and the available data.

The water is reaching the groundwater table after precipitation and infiltration cause level changes in the table. The main principle behind the water table fluctuation (WTF) method is rising water level due to the recharge event (Healy & Scanlon, 2010). In the WTF method, the recharge can be calculated the specific yield and rise of the water level in the observed well.

$$R = \Delta H_{GW} * Sy \quad (2.8)$$

Where R is recharge (L), ΔH_{GW} (L) is the term of groundwater table rising in time, and Sy is specific yield (dimensionless) (Healy & Cook, 2002). Changes in groundwater level in unconfined aquifer form the basis of the water table fluctuation method, where it results from recharging to the groundwater table. One negative consequence of this method's charging estimates is that it establishes the relationship between precipitation and recharging, and it is defined as ΔH_{GW}. Between the recharge events, the recession due to several reasons like evaporation, discharge, and/or lateral transport in saturated media may occur while recharging. Consequently, the real ΔH_{GW} is higher than the height between the lowest and highest points of water level of the examined recharge event. In other words, in the absence of an episode of precipitation, there will be a difference in ΔH_{GW} due to the reduction in the groundwater table. This difference causes lower estimations on recharge. The master recession curve (MRC) is used to estimate the height of the groundwater level in the absence of recharge (recession). The MRC code estimates the water table level in the time step of recession with extrapolations that parameters are defined by the user. Then, recharge is calculated with the difference of extrapolated groundwater level and highest water level (Real ΔH_{GW}) multiplied by the specific yield (Heppner & Nimmo, 2005).

Another method for implementing the WTF method is the RISE method. In this method, the daily rise of the water level and its difference from the previous day are recorded (at fixed time intervals). If there is no difference (or is in the negative direction), the data is recorded as zero that day. This method does not consider recession (Delin et al., 2007; Nimmo et al., 2015; Yang et al., 2018).

Unlike the RISE method, the estimation of recharge using the graphical approach to the WTF method works not at certain time intervals, but in hydrological episodes. It

also predicts the groundwater drop due to recession as in the master recession curve (MRC) method. In this method, extrapolation is done manually; users may draw the recession curves differently (Delin et al., 2007; Delottier et al., 2018; Nimmo et al., 2015). Like the RISE method, the graphical approach does not define the precipitation amount that caused the change of water table level (Nimmo et al., 2015; Nimmo & Perkins, 2018).

The episodic master recession (EMR) (Allocca et al., 2015; Mitchell et al., 2014; Nimmo & Perkins, 2018) method defines discrete recharge episodes based on WTF rates. It estimates recharge by identifying with a cause-and-effect relationship of water input for each episode. The codes of EMR and MRC are designed in the R language in R software that can be downloaded free from www.r-project.org.

The method starts with the master recession curve (MRC), a function for the relation between the height of the water table, H, and decline rate, dH/dt (Delin et al., 2007; Heppner & Nimmo, 2005). MRC is useful for predicting the tendency on the rate of change of water table with time when there is no recharge. It detects the slope elements that describe the short intervals that occur during the recession when there is no precipitation (Nimmo & Perkins, 2018). The unique MRC equation of the well reveals the decline rate of water level with a linear equation.

The input data file for MRC includes time, hydrograph data (for each year; in this study, 2018 and 2019 hydrograph data were used), and cumulative precipitation data, which was obtained from MétéoFrance. There are several parameters required for MRC, as shown in Table 2.3 and Table 2.4. The parameters in the code, mindrytime (which is related to how fast response the well), maxdelprec (the amount of precipitation that is accepted as negligible), tslength (length of slope elements), maxtick (maximum uptick for a linearized slope element), and binsize (for binning the dH/dt in the graph) are defined to represent recession data. That is, it should be created to cover periods without recharging. The best way to find the closest parameters is by trial and error. The output of code includes the graph shows points of the decline of hydrograph according to time (The chart of H to dH/dt) and the best fit linear equation of MRC (the recession parameters created by MRC code); after the user-defined parameters are identified, the decline rate of slope elements is revealed with linear

regression. Each slope elements' midpoint and their water level values are paired in the graph. The linear equation of MRC is fitted to these points.

The episodic master recharge (EMR) approach uses the MRC fitted equation in both forward and backward extrapolations of water table rise, as seen on Figure 2.4.

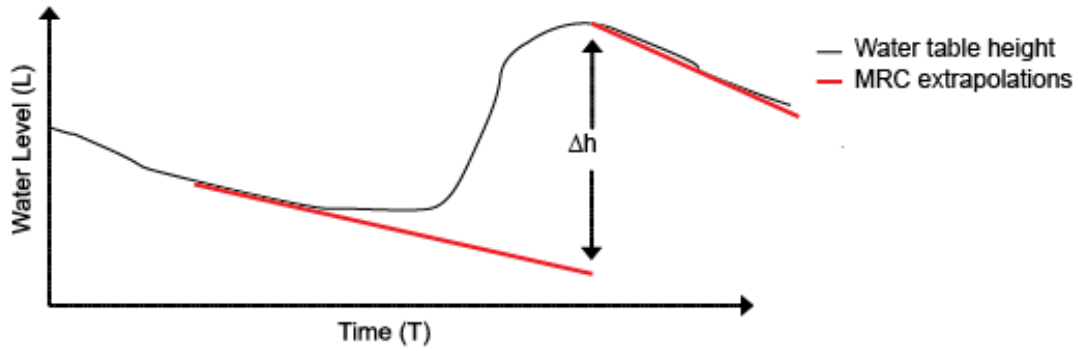

Figure 2.4. Determination of the water table fluctuation with MRC extrapolations (Modified from Delottier et al. (2018))

With the output data of the MRC code, EMR defines the events of recharges with separated events and calculates the recharges for each episode. The inputs of EMR calculation are (1) hydrograph data with time, (2) cumulative precipitation like the MRC method. Also, specific yield (capacity) is needed, as seen in equation 8. All of the parameters appearing in the tables except capacity were obtained by the trial-and-error method and by interpreting the characteristics of the study area in order to create the appropriate episodes. The other important parameter is fluctuation tolerance (fluc_tol) is to prevent insignificant fluctuations in the water table. It can be directly indicative of the measurement noise (Nimmo & Perkins, 2018). It was ensured that the precipitation data were included in the episode sets by exceeding the specified tolerance values. The rate of change of water level lower than fluctuation tolerance is not considered for episodes. The time elapsed between the precipitation event and the change in groundwater is represented by the lag (lag_time), a field-specific parameter. The fact that the lag_time parameter is 2.5 days is not a long time. The reason why this period is short can be interpreted as the well-developed fracture crack system in the aquifer. The parameter is named epend_par is the time value for determining the end of the episode. For water table responses (the other type of input is streamflow data), the time between the top of episode and stabilization on the master recession curve. minprecip is the minimum precipitation limit for precipitation including into episode.

minprecip parameter controls the inclusion of precipitation values below this parameter in the hydrograph response period. In both analyzes, this value was determined as 10 mm. As this value increases, the number of episodes decreases, or by ignoring this parameter (if a negative value is entered, this parameter will not work), all precipitation data can be included in the episodes. However, in this case, the results may consist of snowfall melt or other factors. In this study, the minprecip parameter is expressed with a minimum value; The reason for this is to prevent measurement errors caused by the MRC algorithm. Additionally, for data simplification, the points before and after each point are averaged (moving average with smoothing technique). Nsmooth allows selecting the size of the interval to be averaged.

The MRC and EMR calculations for this study were made for 2018 and 2019; the inputs are shown in Table 2.3 and Table 2.4.

Table 2.3. MRC and EMR input for 2018 (d: day, m: meter)

Master Recession Curve		Episodic Master Recession	
mindrytime	1 d	hytype	WT
maxdelprec	1 m	capacity	0.02
tslength	3 d	lag_time	2.5 d
maxtick	0.3 m	fluc_tol	0.025 m/d
bin size	0	minprecip	10 mm
		epend_par	1.8 d
		nsmooth	0

Table 2.4. MRC and EMR input for 2019

Master Recession Curve		Episodic Master Recession	
mindrytime	2 d	hytype	WT
maxdelprec	1 m	capacity	0.02
tslength	4 d	lag_time	2.5 d
maxtick	0.2 m	fluc_tol	0.003 m/d,
bin size	0	minprecip	10 mm
		epend_par	1.5 d
		nsmooth	0

Daily rainfall amount (mm), daily evapotranspiration (mm), and daily temperature data for the period of 01/1990 – 12/2020 were provided by the MétéoFrance Beauvais-

Tille station at a distance of 4.5 km from the study area. A CTD Diver obtained the daily water table measurements from PZ-1 for MRC, and EMR approaches for the period of 01/2018 to 12/2019 (Schlumberger Water Services, 2014).

2.3. Numerical Modelling

The numerical groundwater model is created for understanding the groundwater flow, distribution of hydraulic properties of the study area. In this study, Groundwater Vistas 8, a user-friendly pre and post-processor software for numerical simulations in MODFLOW models, was used as a graphical user interface (GUI) software (Rumbaugh & Rumbaugh, 2020).

The geostatistical studies as interpolations were studied with the Surfer software (Golden Software LLC, 2021). The interpolation method was selected as kriging. All surfer maps in this study have 100 rows and 87 columns.

The model grid was designed with block centered finite difference technique. A grid of 2500 cells (total and active cells) was created with 50 rows, 50 columns; the grid spacings were 2.6 m and 2.28 m for rows and columns, respectively. The model, which comprises about 14820 m2 area, was created as a single layer. As stated in Groundwater Vistas (GV) manual (Rumbaugh & Rumbaugh, 2020), the coordinate system of the site which was used in Surfer studies (Lambert I), and the model grid which was created with finite difference technique were different. To prevent this difference, the offset values were inputted for orientation.

Numerous parameters are associated with the definition of the boundary conditions around the experimental site. These are the piezometric head, direction of flow, transport parameters, geometrical reconstruction of the aquifer (top and bottom of aquifer, thickness), hydrologic stresses, leakage, and conductance (Zghibi et al., 2015; Zouhri et al., 2009). These boundary conditions were determined by the piezometric data. The interpolation map of piezometric heads around the study area was used as general head boundaries for the model; these boundaries were accepted as fixed-head boundaries.

The steady-state model was created with hydraulic head measurements of the study area in May-2021. Then, the hydraulic conductivity of the area was estimated using the parameter estimate tool (PEST) (Doherty, 2010), which is a valuable inverse modeling. The calibration procedure was followed with using the pilot point technique. The heterogeneous distribution of hydraulic conductivity was estimated using pilot points created with quick pilots (regular grid). After several calibrations with the PEST tool, the other parameters such as recharge calculated with the EMR method (2019 result), specific yield, and porosity were entered. The specific yield and porosity values of 0.02 and 0.30, respectively, were assigned uniformly to all area. These values are within the range of values in published literature sources for chalk aquifer and study area (Crampon et al., 1996). Then, the PEST tool was rerun, and the best possible calibration has been achieved.

The transient model of the study area was created with the piezometric data that was observed in May-2021 and August-2021. All available wells were measured, and a transient model was created with the steady-state model; the initial head data from the steady-state model were used. Two stress periods were created; the first period's length was one day with one time step, and the second was 100 days with 20-time steps. Since an average of 30 cm regression was observed in the piezometric measurements made in the wells, the boundary conditions were transformed into a transient model with a 30 cm decrease. Hydraulic conductivity estimation was generated with the transient model of the study area with the estimations made with the PEST tool.

3. RESULTS

3.1. Slug Test Results

Several types of responses after slug test initiations were recorded and can be seen for each well in the

APPENDIX. The downward movements of water level in the test wells within the recommended normalized head ranges of the Bouwer and Rice method seem as predicted. The dashed lines in the graphs represent lower and upper limits of recommended normalized head ranges of the method. The water responses over time and the Bouwer & Rice solution fitted quite well in the test of F-4, F-5, PZ-2, PZ-3, PZ-4, PZ-5, PZ-8, and PZ-14. The late time of experimental curves of F-5 PZ-8 and PZ-14 tests showed the slow downward movement to the equilibrium (long tailing). Close and consistent results were obtained in the tests performed on PZ-2, PZ-3, PZ-4, and PZ-5.

The result graphs of F-1, F-3, PZ-7, PZ-9, PZ-10, and PZ-13 may have double straight line effects (Bouwer, 1989). However, the slope angles of tests that were implemented on F-1, F-3, and PZ-9 were different from PZ-7, PZ-10, and PZ-13. After the injection of water in the F-1, F-3, and PZ-9, a rapid decrease in the water table and then a slower decrease in this rate was observed; in the PZ-7, PZ-10, and PZ-13, a slow decrease and then a faster decrease was observed than before. These two behaviors, which are different from each other, can be associated with the drilling technique and well development processes used during the drilling of the wells. There can be negative well skin effect in the mentioned first set, and positive well skin effect in the second set.

Another remarkable result is the equilibrium attainment behavior that changes as successive experiments are performed in PZ-7, PZ-10, and PZ-13. It was observed that the water table reached equilibrium more quickly as the number of experiments in the

well increased. This behavior can be associated with removing the fine-grained material present in the well wall by pushing it towards the aquifer during the experiment. Thus, the water table rising with the water injected into the well during the test may have reached equilibrium more quickly than seen in previous experiments. On the other hand, the opposite behaviors were observed in the PZ-9. It is thought that a thick skin layer in these wells may be effective in reducing the pressure towards the aquifer.

The experimental results of slug tests on FC, PZ-1, PZ-6, and PZ-12 were inconsistent with each test on the wells. The reason for inconsistency may be occurred due to the well skin effect. When analytical solutions were made, similar and consistent results could not be obtained as in other wells. The fitting procedure on AQTESOLV could not be implemented on the tests on PZ-12, Test-18 on PZ-9, and Test-34 on FC, because while injecting water into the wells, overflows were observed that might affect the calculations.

Table 3.3 shows the experimental results of slug tests which were calculated by using AQTESOLV. As seen on the table, the hydraulic conductivity values range from 4.43e-08 to 7.56e-06 m/s.

3.2. Recharge Calculations

The method was implemented with 2018 and 2019 water level and precipitation data with no gaps between 1 January 2018 to 31 December 2019 and was evaluated separately. Figure 3.1.a and Figure 3.2.a show the cumulative precipitation with water table level. The blue crosses represent the start of the recession. The red points figure the period of recession. Recession starts and periods seen in the graph were tried to be arranged to overlap with the cumulative precipitation data. That shows the water table shows a quick response to precipitations.

Figure 3.1.b and Figure 3.2.b show the MRC curve created with the best-fitted curve to the recession data. The blue squares on the water level graph, H(t), and the calculated rate of change, dH/dt, represent the slope of the regression of the water table

at the given level. If the selected slopes need to be separated, the bin average MRC method explained by Heppner and Nimmo (2005) can be used to simplify the data.

Figure 3.1.c and Figure 3.2.c, respectively for 2018 and 2019, show the EMR results of the dataset with using the MRC equations and other parameters listed in Table 2.3 and Table 2.4. The water table level and cumulative precipitation data are shown. The bold blue columns represent the recharge periods. Red lines figure the MRC extrapolations. Multiplication of the difference of extrapolations and specific yield gives the recharge value for the specified episode. All recharge estimations for each episode are shown in Table 3.1 for 2018 and Table 3.2 for 2019.

Total recharge values are 106,87 mm and 106,49 mm for 2018 and 2019, respectively.

Table 3.1. Water table episodes table (2018)

Episode	Start time (d)	Duration (d)	Start (m)	End (m)	Difference (m)	Episode recharge (mm)
1	12	66	72.26	74.29	2.03	56.01
2	84	45	74.26	74.1	-0.17	13.21
3	144	18	73.83	74.22	0.39	13.85
4	219	6	73.09	73.11	0.02	2.13
5	313	7	72.09	72.15	0.05	2.7
6	321	10	71.99	72.16	0.17	5.83
7	332	3	72.06	72.13	0.07	2.08
8	337	13	71.99	72.39	0.4	11.06
					Sum (mm/year)	106.87

Table 3.2. Water table episodes table (2019)

Episode	Start time (d)	Duration (d)	Start (m)	End (m)	Difference (m)	Episode recharge (mm)
1	25	11	72.56	72.72	0.16	7.15
2	37	14	72.7	72.96	0.26	10.02
3	57	22	72.9	73.34	0.44	16.3
4	97	3	73.24	73.28	0.04	1.78
5	116	3	73.02	73.06	0.04	1.8
6	120	6	72.99	72.97	-0.01	1.72
7	130	5	72.87	72.89	0.02	2.06
8	152	7	72.35	72.47	0.11	4.88
9	207	17	71.78	72.24	0.46	16.07
10	225	14	71.81	72.17	0.36	12.84
11	269	8	71.5	71.54	0.05	4.24
12	288	17	71.41	71.71	0.3	13.21
13	306	10	71.59	71.78	0.19	7.92
14	317	8	71.71	71.88	0.16	6.51
					Sum (mm/year)	106.49

Table 3.3. Hydraulic conductivity values after slug tests, calculated with AQTESOLV

Test No	Date	Injection	M. Freq	K (AQTESOLV) (m/s)
Test-1	03.03.2021	F-4	30 sec	-
Test-2	10.03.2021	F-4	min	7.192e-7
Test-3	26.03.2021	F-4	min	6.602e-7
Test-4	30.03.2021	PZ-13	sec	8.583e-7
Test-5	07.04.2021	PZ-13	sec	1.317e-6
Test-6	09.04.2021	F-5	sec	1.831e-6
Test-7	09.04.2021	F-5	sec	1.674e-6
Test-8	12.04.2021	F-5	sec	1.531e-6
Test-9	13.04.2021	PZ-14	sec	2.275e-6
Test-10	14.04.2021	PZ-14	sec	2.869e-6
Test-11	15.04.2021	PZ-14	sec	2.170e-6
Test-12	16.04.2021	PZ-10	sec	1.335e-6
Test-13	16.04.2021	PZ-10	sec	1.489e-6
Test-14	19.04.2021	PZ-10	sec	1.613e-6
Test-15	20.04.2021	PZ-12	sec	PROBLEM
Test-16	20.04.2021	PZ-12	sec	PROBLEM
Test-17	21.04.2021	PZ-12	sec	PROBLEM
Test-18	22.04.2021	PZ-9	sec	PROBLEM
Test-19	23.04.2021	PZ-9	sec	7.961e-8
Test-20	23.04.2021	PZ-9	sec	8.799e-8
Test-21	23.04.2021	PZ-9	sec	8.953e-8
Test-22	10.05.2021	PZ-8	sec	2.348e-6
Test-23	10.05.2021	PZ-8	sec	2.356e-6
Test-24	11.05.2021	PZ-8	sec	2.355e-6
Test-25	12.05.2021	F-4	2sec	6.593e-7
Test-26	12.05.2021	F-4	2sec	6.321e-7
Test-27	12.05.2021	F-4	2sec	6.750e-7
Test-28	17.05.2021	PZ-13	2sec	2.981e-6
Test-29	17.05.2021	PZ-13	2sec	2.935e-6
Test-30	17.05.2021	PZ-13	2sec	2.892e-6

Test No	Date	Injection	M. Freq	K (AQTESOLV) (m/s)
Test-31	19.05.2021	PZ-7	2sec	6.383e-6
Test-32	19.05.2021	PZ-7	2sec	7.164e-6
Test-33	19.05.2021	PZ-7	2sec	7.56e-6
Test-34	20.05.2021	FC	2sec	PROBLEM
Test-35	20.05.2021	FC	2sec	4.889e-8
Test-36	20.05.2021	FC	2sec	2.718e-7
Test-37	21.05.2021	PZ-6	2sec	1.844e-6
Test-38	21.05.2021	PZ-6	2sec	1.809e-6
Test-39	21.05.2021	PZ-6	2sec	2.095e-6
Test-40	25.05.2021	F-3	2sec	4.427e-8
Test-41	25.05.2021	F-3	2sec	7.623e-8
Test-42	26.05.2021	F-3	2sec	7.961e-8
Test-43	26.05.2021	PZ-5	2sec	2.299e-6
Test-44	26.05.2021	PZ-5	2sec	2.859e-6
Test-45	27.05.2021	PZ-5	2sec	2.818e-6
Test-46	28.05.2021	PZ-1	2sec	4.701e-6
Test-47	28.05.2021	PZ-1	2sec	6.567e-6
Test-48	31.05.2021	PZ-1	2sec	5.957e-6
Test-49	01.06.2021	PZ-3	2sec	2.121e-7
Test-50	01.06.2021	PZ-3	2sec	2.024e-7
Test-51	01.06.2021	PZ-3	2sec	2.03e-7
Test-52	02.06.2021	F-1	2sec	1.502e-7
Test-53	02.06.2021	F-1	2sec	1.231e-7
Test-54	03.06.2021	F-1	2sec	1.124e-7
Test-55	03.06.2021	PZ-2	2sec	3.597e-7
Test-56	04.06.2021	PZ-2	2sec	3.396e-7
Test-57	07.06.2021	PZ-2	2sec	3.29e-7
Test-58	08.06.2021	PZ-4	2sec	1.109e-7
Test-59	08.06.2021	PZ-4	2sec	1.1e-7
Test-60	09.06.2021	PZ-4	2sec	1.164e-7

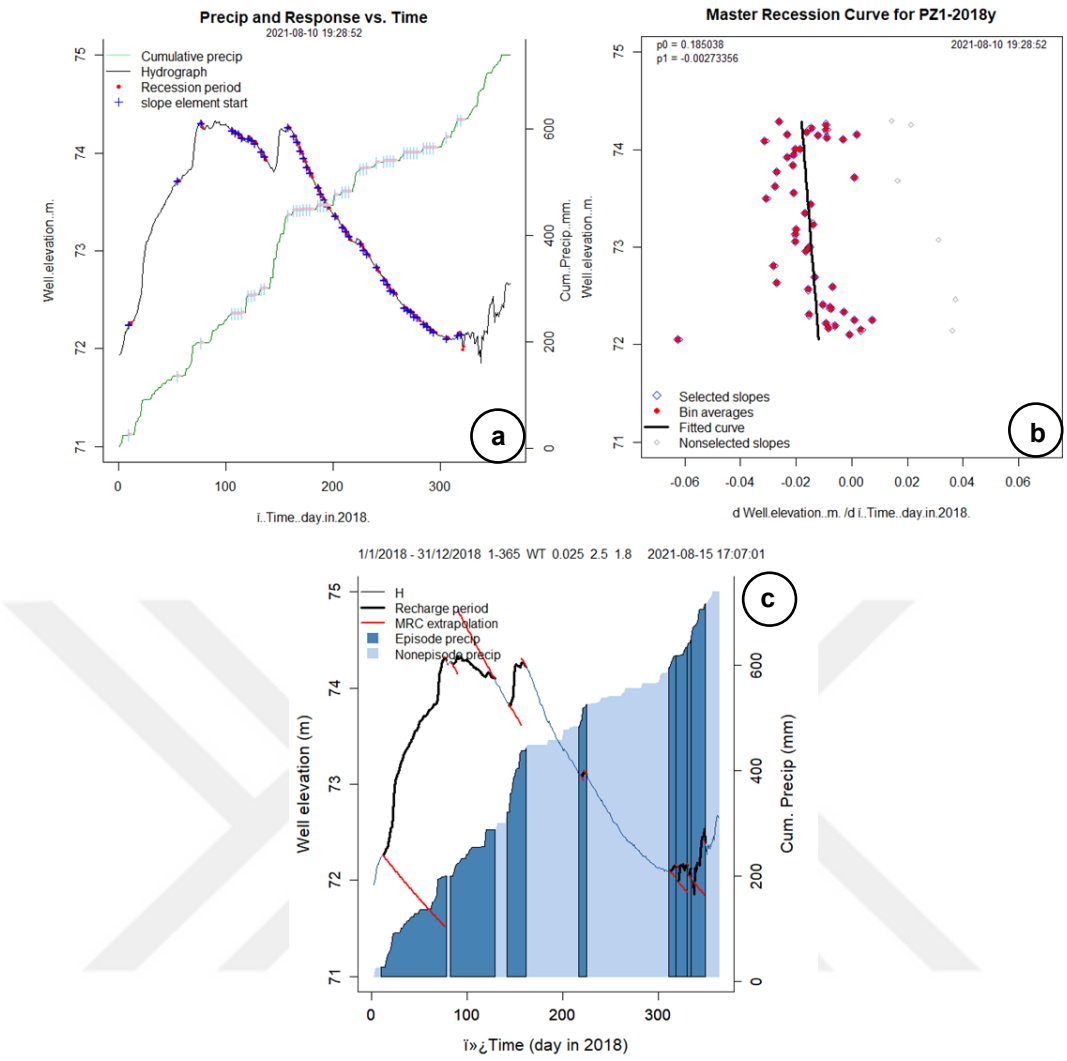

Figure 3.1. MRC and EMR graphs for 2018 a. Cumulative precipitation and water level b. Distribution of recessions for MRC equation c. Episodic recharge period

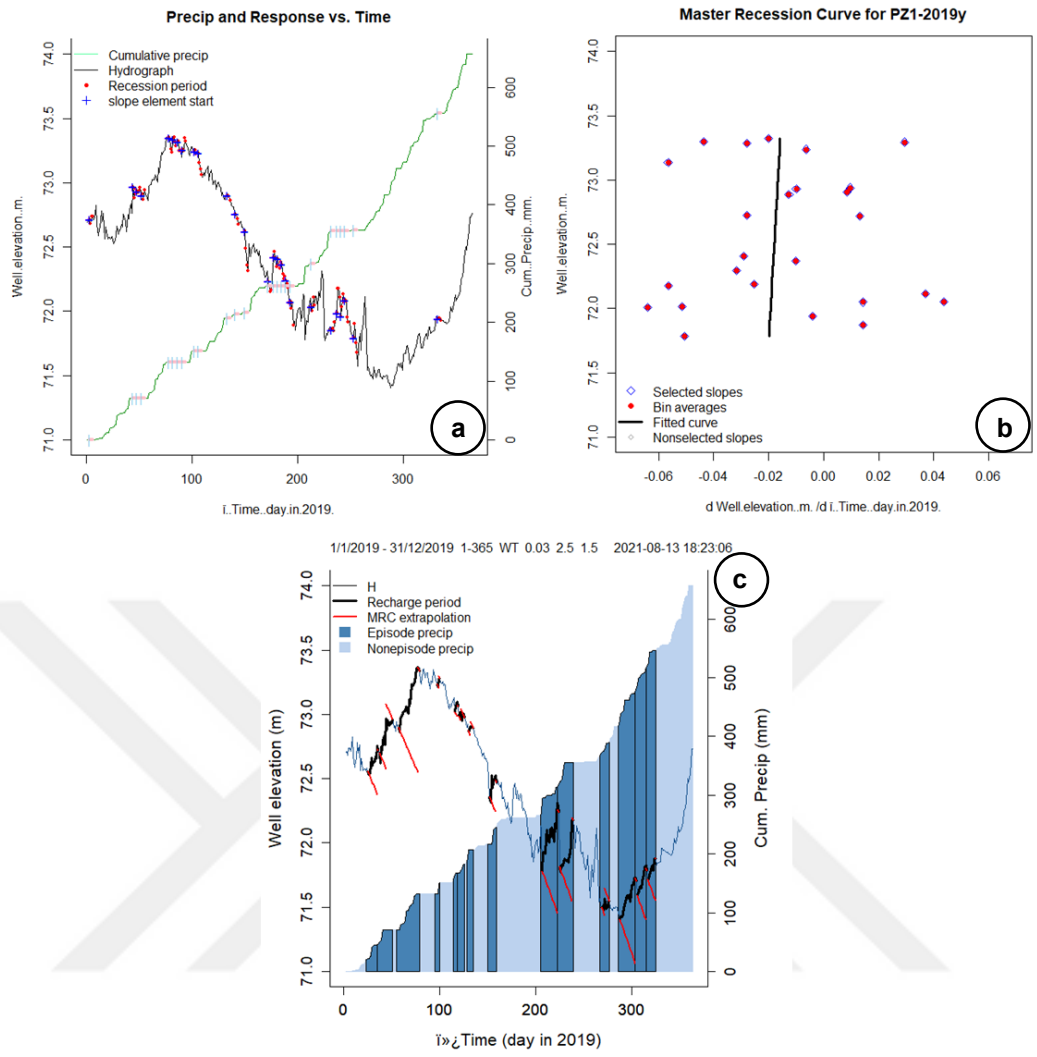

Figure 3.2. MRC and EMR graphs for 2019 a. Cumulative precipitation and water level b. Distribution of recessions for MRC equation c. Episodic recharge periods

3.3. Model Results

The piezometric head values of the wells in the study area were measured, and the interpolation map based on the kriging technique was created (Figure 3.3). Also, hydraulic conductivity values obtained from slug tests were interpolated with the same technique, and the interpolation map was created, as seen on Figure 3.4. The grid data in each map were multiplied and overlayed to create a transmissivity map of observations (Figure 3.5). The transmissivity values range between 4.85e-06 and 4.99e-04 m^2/s.

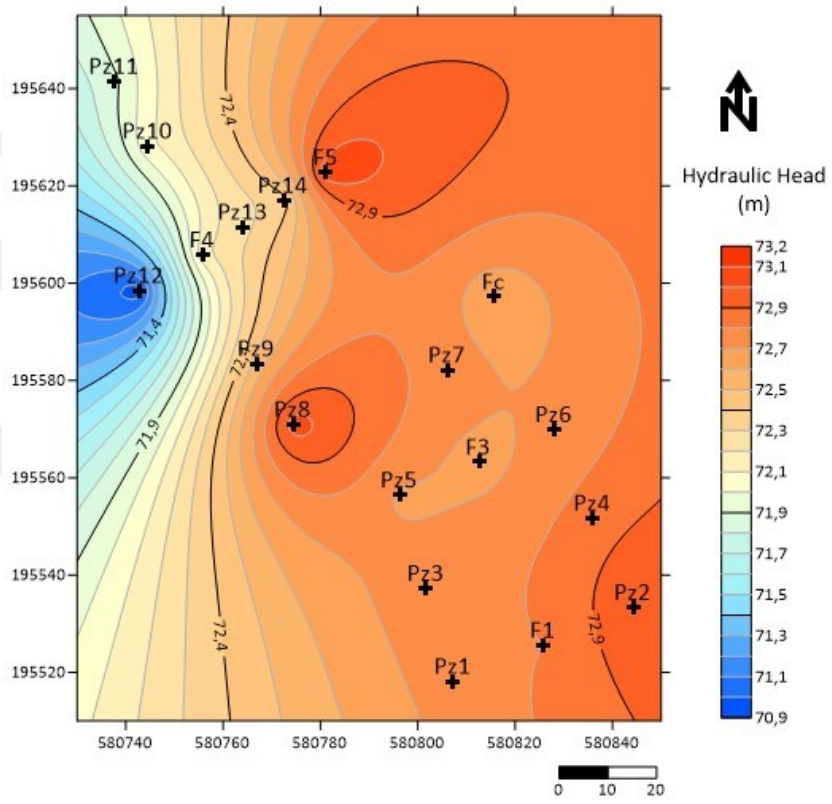

Figure 3.3. Measured piezometric levels

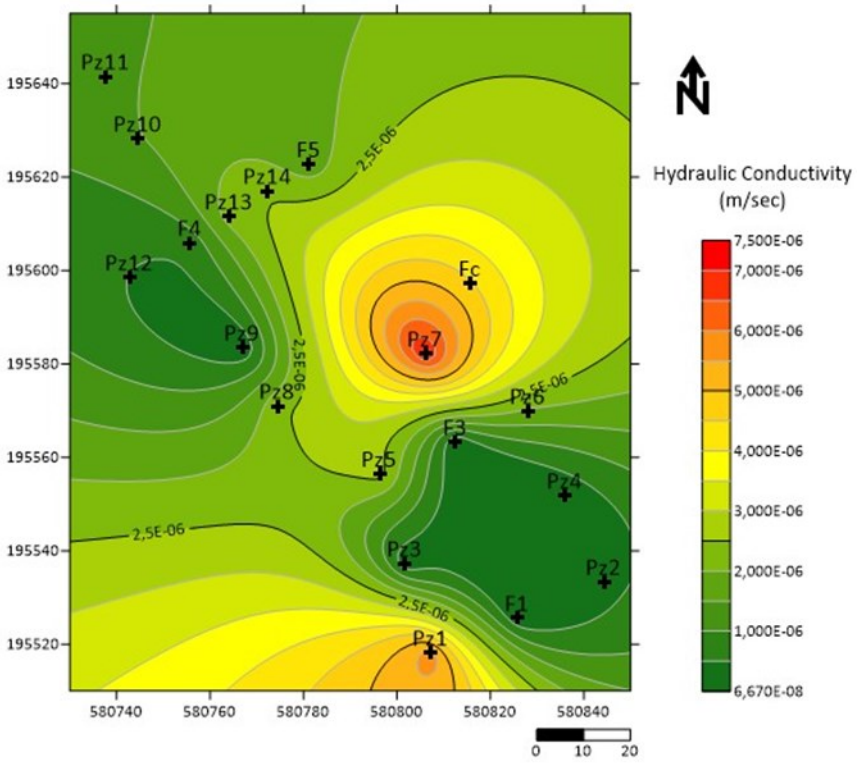

Figure 3.4. Hydraulic conductivity values obtained from slug tests

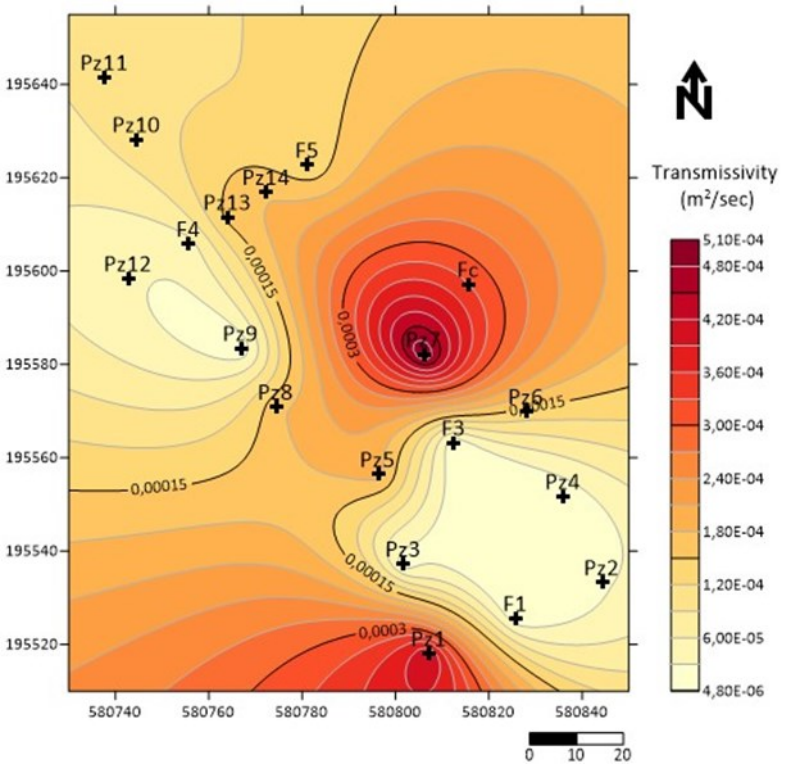

Figure 3.5. Transmissivity map, created with overlaying the piezometric head and hydraulic conductivity maps

As written on chapter 2.3, the general boundaries were assigned from interpolation of the piezometric map seen on Figure 3.3. By examining the grid data of the interpolation map, boundary conditions at the edges of the model were determined. Numerical model created with the grid and parameters described in the related section, the calibration results of the model for steady-state conditions are as seen on Table 3.2, and Figure 3.6 shows the calibration graph with observed and computed values:

Table 3.2. Steady-state model calibration statistics

Residual Sum of Squares	1.20e-01
RMS Error	0.08
Minimum Residual	-0.06
Maximum Residual	0.31
Range of Observations	1.17

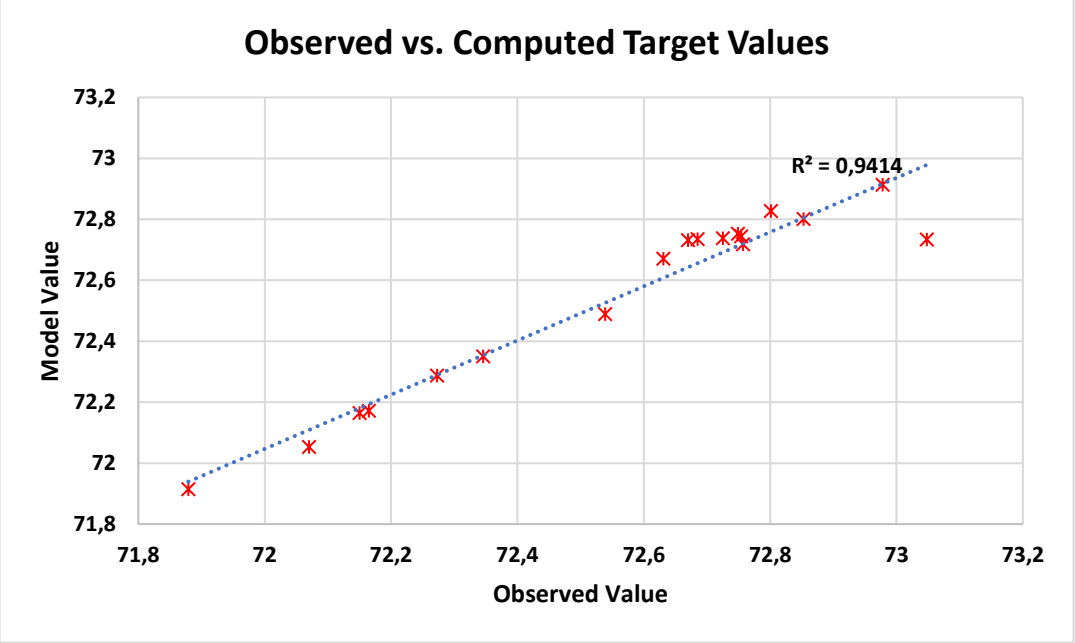

Figure 3.6. The calibration graph of the steady-state model

The RMS Error (Root mean square error) measures the distance between the data points from the regression line. In the steady-state calibration the RMS error is 0.08 m.

Regarding the volumetric water budget of the steady-state model, it is seen on Table 3.3 that there is a daily water flow of 74 m^3 in the aquifer. This makes sense, given the

hydraulic conductivity and flow gradient of the aquifer. The discrepancy between the mass entering and leaving the system is 0.44%.

Table 3.3. Volumetric water budget of steady-state model for one day

	Constant Head	Recharge
In (m^3 / day)	69.9217	3.9821
Out (m^3 / day)	74.2260	
In - Out (m^3 / day)	-0.3222	
Discrepancy (%)	-0.44	

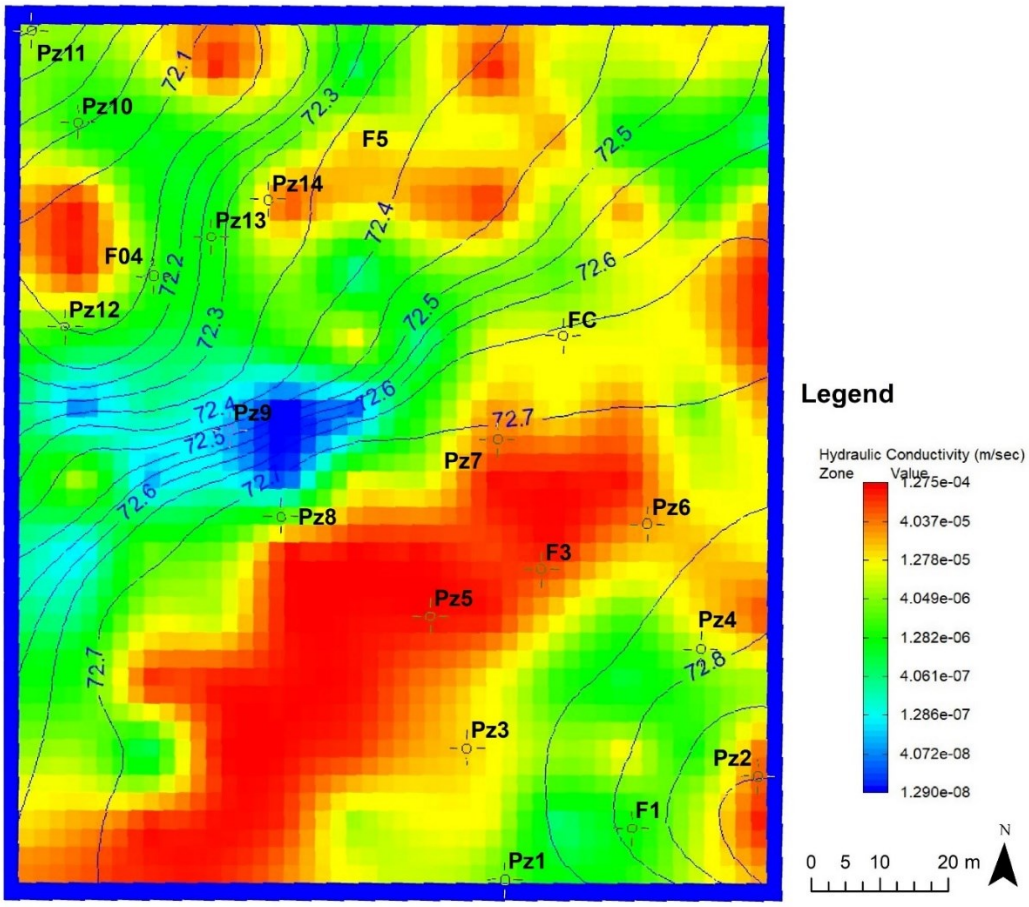

Figure 3.7. Hydraulic conductivity distribution map of the study area (Steady-State)

The grid data of the hydraulic conductivity was exported as a matrix table. The matrix data is a dataset of 2500 cells as expected as the number of cells created in Groundwater Vistas 8. It was imported to the Surfer to create the transmissivity map

with coordinate data. Kriging technique was applied to create the hydraulic conductivity map seen on Figure 3.8.

The transmissivity map seen on Figure 3.9 was created with the multiplication of hydraulic conductivity map data (Figure 3.8) and measured piezometric head data (Figure 3.3).

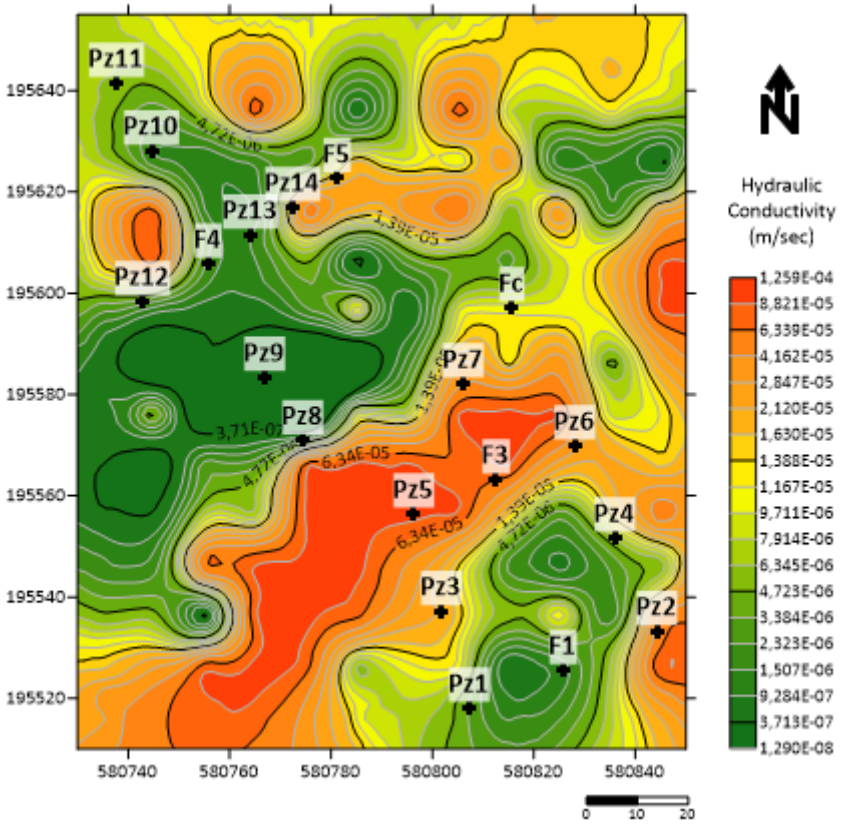

Figure 3.8. Hydraulic conductivity distribution map on Surfer (Steady-State)

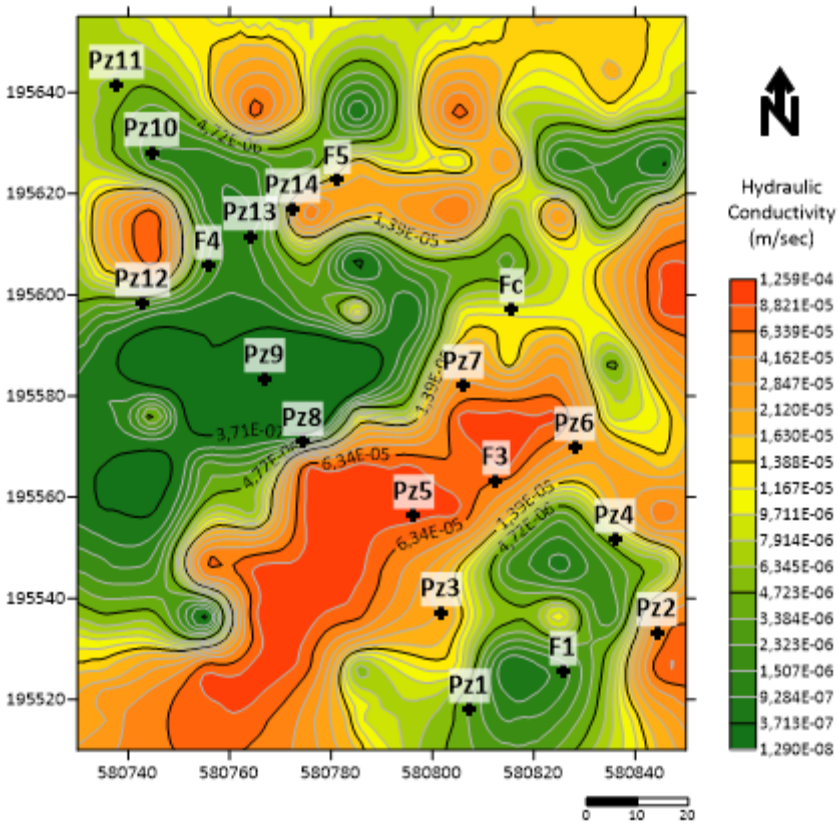

Figure 3.9. Transmissivity map on Surfer (Steady-State)

The transient state calibration statistics are seen on Table 3.4, and Figure 3.10 shows the calibration graph with observed and computed values.

Table 3.4. Transient-state model calibration statistics

Residual Sum of Squares	2.18e+00
RMS Error	0.25
Minimum Residual	-0.20
Maximum Residual	0.64
Range of Observations	1.47

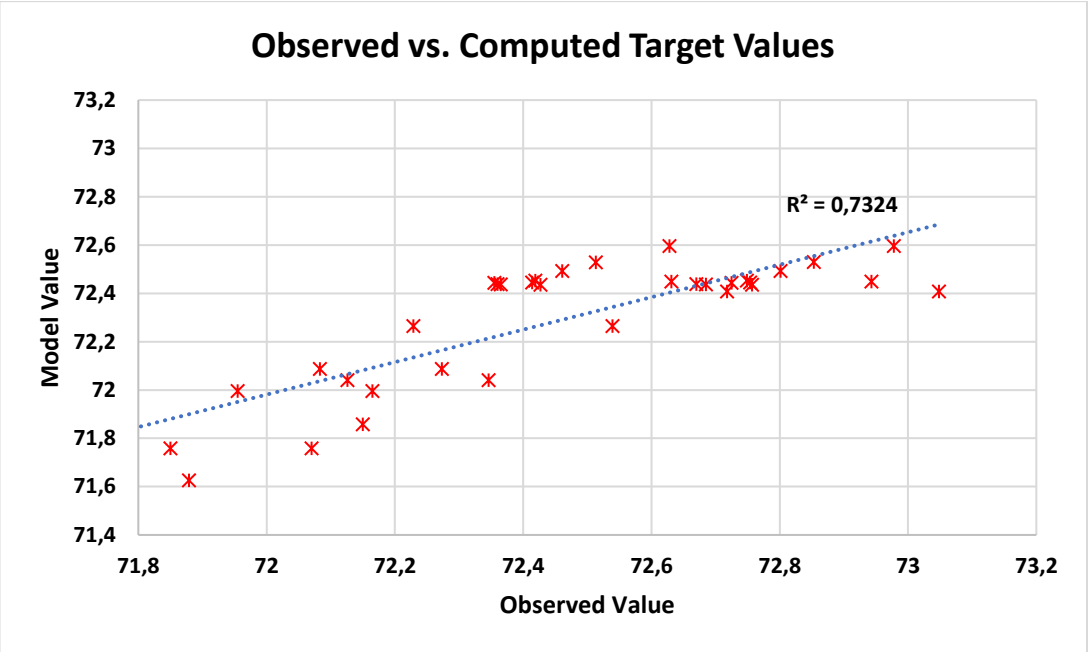

Figure 3.10. The calibration graph of the transient-state model

At the end of the stress periods which were set as 2 periods and a total of 100-days, the water budget calculation of the model can be seen on Table 3.5. The discrepancy between the input and output of water in the system is 1.36%.

Table 3.5. Volumetric water budget of transient-state model for 100-day

	Constant Head	Recharge	Storage
In (m^3 / 100-day)	4030.98	402.19	1.59e-02
Out (m^3 / 100-day)	4493.97		
In - Out (m^3 / 100-day)	-60.78		
Discrepancy (%)	-1.36		

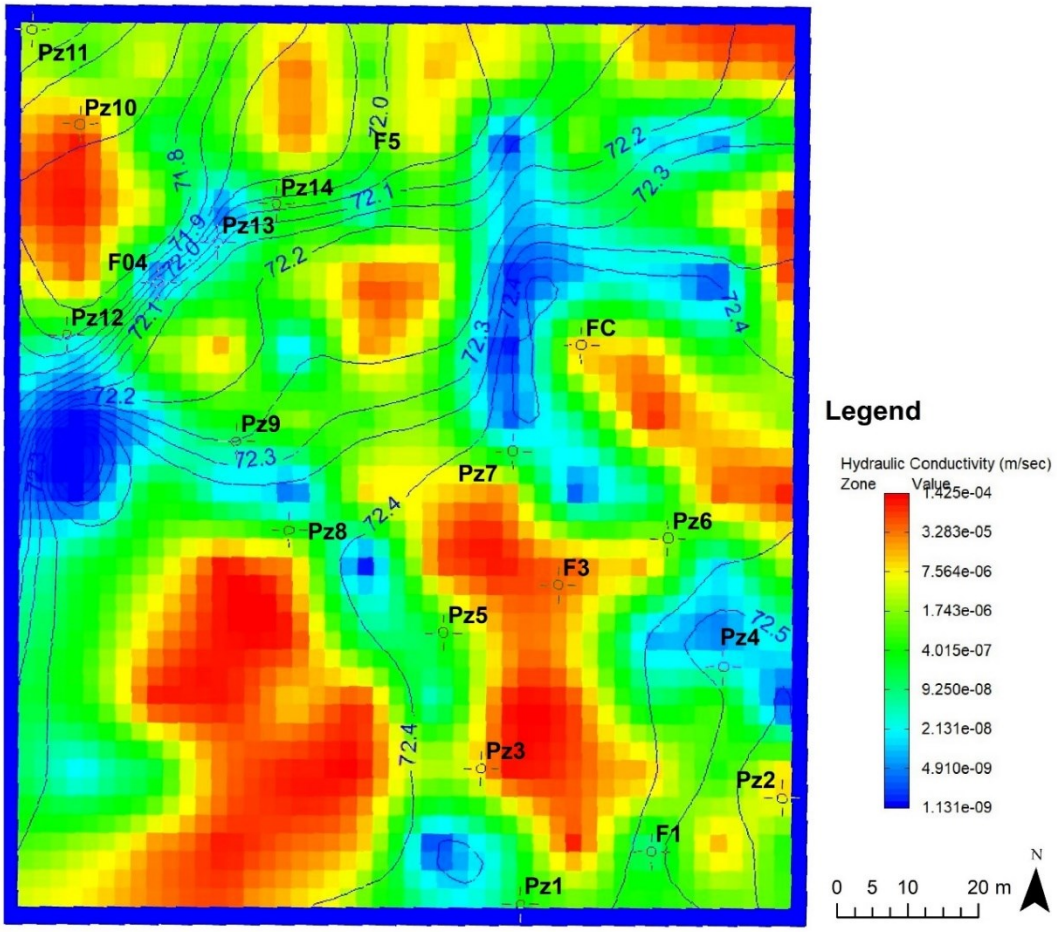

Figure 3.11. Hydraulic conductivity distribution map of the study area (Transient State)

The procedure applied in steady-state conditions was also applied in transient state conditions. The grid data of hydraulic conductivity in 2500 cells were imported to Surfer. The hydraulic conductivity distribution in the transient state was exported with coordinate data can be seen on Figure 3.12.

The transmissivity map seen on Figure 3.13 was created with the multiplication of hydraulic conductivity map data (Figure 3.12) and measured piezometric head data (Figure 3.3).

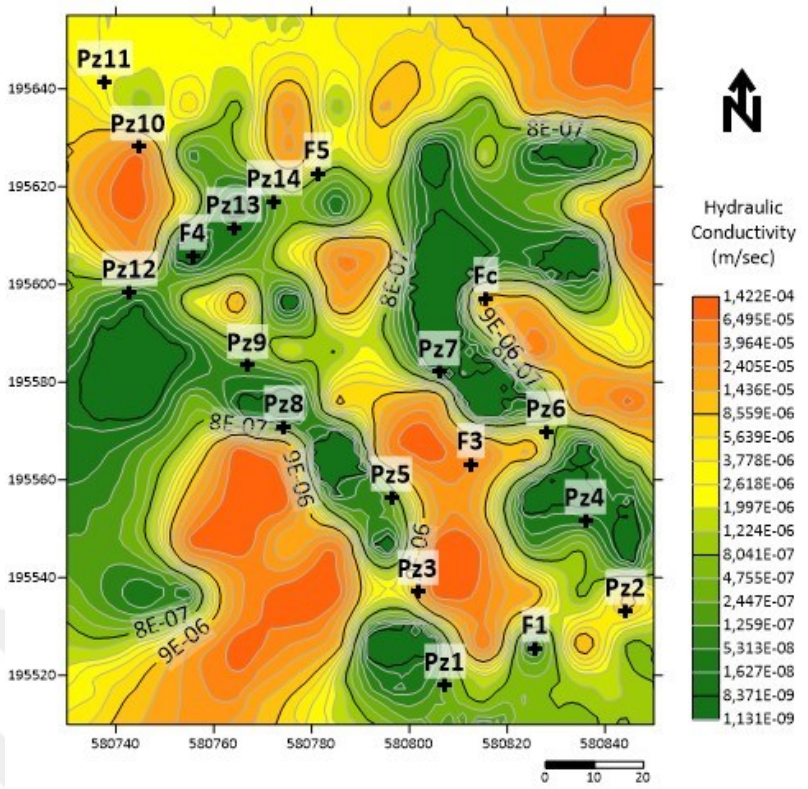

Figure 3.12. Hydraulic conductivity distribution map on Surfer (Transient-State)

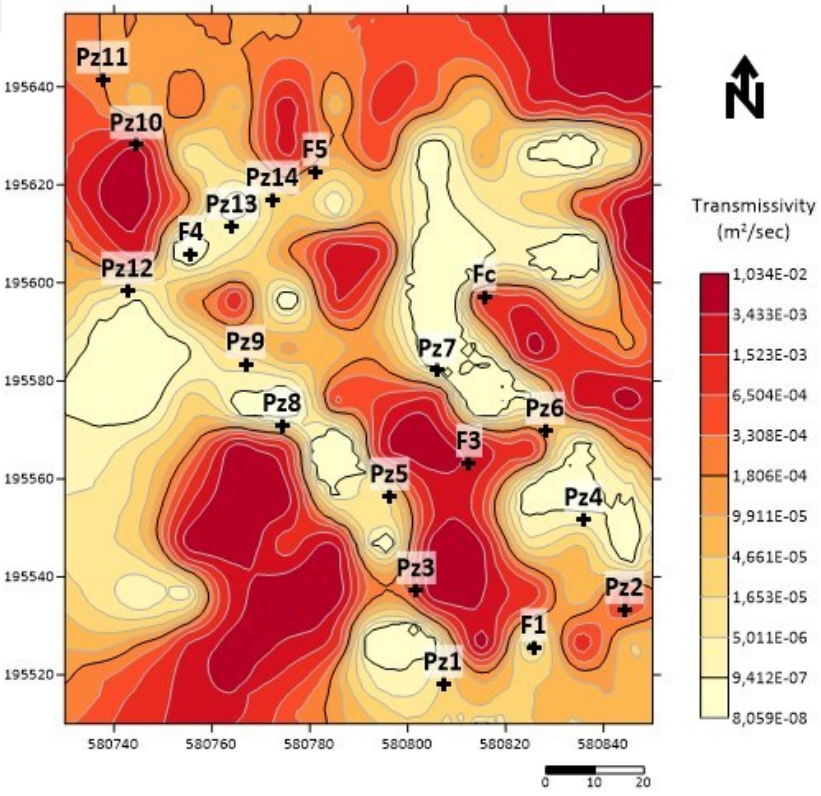

Figure 3.13. Transmissivity map on Surfer (Transient-State)

4. CONCLUSION

The hydrogeological properties of aquifers can be evaluated by hydrogeological investigations in the field and by numerical modelling. The slug test method is one of them and can be preferred due to several advantages. To define it simply, it is the measurement of the water injected into the well to reach a static water level over time. There are many methods for analyzing the slug test data. In this study, the Bouwer and Rice (1976) method was applied by using AQTESOLV (Duffield, 2007). A data set was created by performing a minimum of three experiments in the wells in the experimental site, and hydraulic conductivity values were calculated with analytical analysis. The analytical results showed large differences between the wells; the heterogeneity of the study area can explain this situation.

Moreover, there is uncertainty about slug tests explained in the previous studies. The hydraulic conductivity estimations from the slug test are appreciably lower than hydraulic conductivity achieved from the pump test (Butler & Healey, 1998). As Butler (2019) stated, the discrepancy between the slug test and other field tests can be explained by the length of the effective radius. Also, as Ii and Niemann (2001) stated, well skin can influence the hydraulic conductivity values obtained by slug test analysis to overestimate or underestimate according to the technique of well development. If there is an area around the well with hydraulic conductivity lower than the hydraulic conductivity of the aquifer, usually due to the drilling technique, it refers to positive well-skin, underestimation is expected. On the other hand, in wells that are overdeveloped such that this surface of a well has a higher hydraulic conductivity from the aquifer, it is called as negative well-skin, overestimation is expected (Yeh & Chen, 2007). In addition, the relationship between well efficiency and the accuracy of the slug test results is explained by Dennis (1987) shows that as the well efficiency increases, the accuracy of the slug test results increases; if a correction factor for the well efficiency is determined, the aquifer parameters obtained by the slug test represent

a more accurate. Because slug tests, unlike pumping tests, can be excessively influenced by well construction processes. For all these reasons, there can be significant variations in analytical solutions between wells.

On the other hand, necessary hydrogeological parameters for the numerical modeling of the study area were determined. Master recession curve (MRC) and episodic master recession (EMR) approaches were used to calculate the recharge. EMR recharge episodes were identified by water table fluctuations and MRC extrapolations, as seen in Figure 3.1.c and Figure 3.2.c. Some minor fluctuations were not included in these episodes as they did not exceed some thresholds in MRC and EMR code parameters (such as latency time and fluctuation tolerance). Since the characteristics of the aquifer cannot be evaluated homogeneously, it may cause errors in the calculations. In this study, the specific yield was taken as 0.02, but it should be noted that this value is within a range in studies conducted in the literature. Different results can be obtained by using site-specific parameters. The resulting recharge values are within the range of values in the published study (Crampon et al., 1993).

Numerical modeling of the study area was done in steady-state and transient state conditions. The calibrations of the observed and modeled values were done with the PEST tool. The calibration statistics express that the normalized root mean square (RMS) for the steady-state model and transient state model are 0.08% and 0.25%, respectively. The calibration of models can be improved with more data from the aquifer, such as new geological interpretation and/or data from pumping tests, with the construction of a new well. As seen on Figure 3.7, the hydraulic conductivity of the area in the steady-state model varies between 1.28e-4 m/s and 1.29e-8 m/s. In the transient state model as seen on Figure 3.11, the heterogeneity of hydraulic conductivity occurs with values ranging from 1.55e-4 to 1.33e-9 m/s.

There are differences between the analytical solution interpolation map in Figure 3.4 and the numerical solution maps in Figure 3.8 and Figure 3.12. In particular, differences are observed in the hydraulic conductivity values and its distributions, which can be noticed from their legends. One reason of this situation may be due to the situations described in the second paragraph of this section. The other is because of kriging technique. More data from the experimental site provide more accurate

geostatistical result. These results can also contribute to development of numerical modelling process. Also, the maps in Figure 3.3, Figure 3.4, and Figure 3.5 were created with the kriging technique. The maps in Figure 3.7 and Figure 3.11 were created with MODFLOW calculations. The matrix data taken from Groundwater Vistas include 2500 cells and was exported to 8700 cells in Surfer. For this reason, in the values seen in the map and the general distributions of the hydraulic conductivity, the difference between the maps created with kriging and the maps created with MODFLOW can be accepted as negligible.

The heterogeneity of the chalk lithology throughout its distribution is a scientific fact. This study was carried out to obtain the hydraulic properties of the chalk aquifer in the Hydrogeological Experimental Site of Beauvais. The results obtained provide an idea about the spatial distribution of the hydrogeological characteristics of the study area. The relationship between well development and slug testing can be interpreted more clearly with the slug tests to be carried out after future well development studies. Besides, further investigations would bring more consistent and powerful results.

REFERENCES

Alfaifi, H. J. (2015). *Comparing slug test methods for unconfined aquifers*.

Allen, D. J., Brewerton, L. J., Coleby, L. M., Gibbs, B. R., Lewis, M. A., MacDonald, A. M., Wagstaff, S. J., & Williams, A. T. (1997). The physical properties of major aquifers in England and Wales. *British Geological Survey*, *Technical*, 312. http://nora.nerc.ac.uk/13137/

Allocca, V., De Vita, P., Manna, F., & Nimmo, J. R. (2015). Groundwater recharge assessment at local and episodic scale in a soil mantled perched karst aquifer in southern Italy. *Journal of Hydrology*, *529*(P3), 843–853. https://doi.org/10.1016/j.jhydrol.2015.08.032

Audouin, O., Bodin, J., Butler, A. P., Mathias, S. A., Gallagher, A. J., Peach, D. W., Williams, A. T., Audouin, O., & Bodin, J. (2008). Cross-borehole slug test analysis in a fractured limestone aquifer. *Journal of Hydrology*, *348*(3–4), 510–523. https://doi.org/10.1016/j.jhydrol.2007.10.021

Baran, N., Lepiller, M., & Mouvet, C. (2008). Agricultural diffuse pollution in a chalk aquifer (Trois Fontaines, France): Influence of pesticide properties and hydrodynamic constraints. *Journal of Hydrology*, *358*(1–2), 56–69. https://doi.org/10.1016/j.jhydrol.2008.05.031

Barhoum, S., Valdès, D., Guérin, R., Marlin, C., Vitale, Q., Benmamar, J., & Gombert, P. (2014). Spatial heterogeneity of high-resolution Chalk groundwater geochemistry - Underground quarry at Saint Martin-le-Noeud, France. *Journal of Hydrology*, *519*(PA), 756–768. https://doi.org/10.1016/j.jhydrol.2014.08.001

Bault, V., Borde, J., Follet, R., Laurent, A., Tourliére, B., avec la collaboration de Leveau, E., & Willefert, V. (2012). *Atlas hydrogéologique numérique de l'Oise*.

Black, J. H. (1978). *Use of the slug test in groundwater investigations*. *March 1978*.

Bloomfield, J. P., Brewerton, L. J., & Allen, D. J. (1995). Regional trends in matrix porosity and dry density of the Chalk of England. *Quarterly Journal of Engineering Geology*, *28*(Suppl. 2). https://doi.org/10.1144/gsl.qjegh.1995.028.s2.04

Bouwer, H. (1989). *The Bouwer and Rice Slug Test - An Update*. 304–309.

Bouwer, H., & Rice, R. C. (1976). *A Slug Test for Determining Hydraulic Conductivity of Unconfined Aquifers With Completely or Partially Penetrating Wells*. *12*(3), 423–428.

Brouyère, S. (2006). Modelling the migration of contaminants through variably

saturated dual-porosity, dual-permeability chalk. *Journal of Contaminant Hydrology*, *82*(3–4), 195–219. https://doi.org/10.1016/j.jconhyd.2005.10.004

Butler, J. J. J. (1996). Slug Tests in Site Characterization: Some Practical Considerations. *Environmental Geosciences*, *3*(3), 154–163.

Butler, J. J. J. (2019). *The Design, Performance, and Analysis of Slug Tests (2019, CRC Press)*.

Butler, J. J. J., & Healey, J. M. (1998). *Relationship between pumping test and slug test parameters : Scale Effect or Artifact ? April*, 305–313.

Cao, F., Jaunat, J., Vergnaud-Ayraud, V., Devau, N., Labasque, T., Guillou, A., Guillaneuf, A., Hubert, J., Aquilina, L., & Ollivier, P. (2020). Heterogeneous behaviour of unconfined Chalk aquifers infer from combination of groundwater residence time, hydrochemistry and hydrodynamic tools. *Journal of Hydrology*, *581*, 1–38. https://doi.org/10.1016/j.jhydrol.2019.124433

Chen, N., Valdes, D., Marlin, C., Blanchoud, H., Guerin, R., Rouelle, M., & Ribstein, P. (2019). Water, nitrate and atrazine transfer through the unsaturated zone of the Chalk aquifer in northern France. *Science of the Total Environment*, *652*, 927–938. https://doi.org/10.1016/j.scitotenv.2018.10.286

Crampon, N., Custodio, E., & Downing, R. A. (1996). The hydrogeology of Western Europe: A basic framework. *Quarterly Journal of Engineering Geology*, *29*(2), 163–180. https://doi.org/10.1144/GSL.QJEGH.1996.029.P2.05

Crampon, N., Roux, J. C., Bracq, P., in collaboration with Delay, F., Lepiller, M., Mary, G., Rasplus, L., & Alcaydé, G. (1993). France. In R. A. Downing, M. Price, & G. P. Jones (Eds.), *The Hydrogeology of the Chalk of the North-West Europe*. Oxford Science Publications.

Dagan, G. (1978). *A Note on Packer, Slug, and Recovery Tests in Unconfined Aquifer*. *14*(5), 929–934.

Defossez, A., Londe, L., Cabon, F., & Roux, P. (2013). *Hydrogeological Aspects during Closure of an Underground LPG Storage*. 1205–1210.

Delin, G. N., Healy, R. W., Lorenz, D. L., & Nimmo, J. R. (2007). Comparison of local- to regional-scale estimates of ground-water recharge in Minnesota, USA. *Journal of Hydrology*, *334*(1–2), 231–249. https://doi.org/10.1016/j.jhydrol.2006.10.010

Delottier, H., Pryet, A., Lemieux, J. M., & Dupuy, A. (2018). Estimating groundwater recharge uncertainty from joint application of an aquifer test and the water-table fluctuation method. *Hydrogeology Journal*, *26*(7), 2495–2505. https://doi.org/10.1007/s10040-018-1790-6

Dennis, T. S. (1987). *The Effect of Well Efficiency on In-Situ Permeability Test Results*.

Doble, R. C., & Crosbie, R. S. (2017). Review: Current and emerging methods for catchment-scale modelling of recharge and evapotranspiration from shallow groundwater. *Hydrogeology Journal*, *25*(1), 3–23. https://doi.org/10.1007/s10040-016-1470-3

Doherty, J. (2010). PEST: Model-Independent Parameter Estimation, User Manual: 5th Edition. *PEST Manual*, *5th Editio*, 279.

Domenico, P. A., & Schwartz, F. W. (1998). *Physical and Chemical Hydrogeology* (Vol. 79). Wiley. http://www.ncbi.nlm.nih.gov/pubmed/6897892

Duffield, G. M. (2007). *AQTESOLV for Windows Version 4.5 User's Guide*. http://www.aqtesolv.com

Duffield, G. M. (2021). *Slug Tests*. http://www.aqtesolv.com/slug-tests/slug-tests.htm

Fabbri, P., Ortombina, M., & Piccinini, L. (2012). Estimation of Hydraulic Conductivity Using the Slug Test Method in a Shallow Aquifer in the Venetian Plain (NE, Italy). *Aqua Mundi*, *3*(2), 125–133. https://doi.org/10.4409/Am-045-12-0048

Fetter, C. W. (2000). *Applied Hydrogeology 4th Edition*.

Gille, E., Elsass, P., & Lapuyade, F. (2002). Atlas hydrogéologique du bassin Rhin-Meuse, Gaize du Cénomanien. *Agence de l'Eau Rhin-Meuse*, *Code 017*.

Golden Software LLC. (2021). *Surfer user's guide*. http://downloads.goldensoftware.com/guides/Surfer17UserGuide.pdf

Greene, E. A., & Shapiro, A. M. (1995). *Methods of Conducting Air-Pressurized Slug Tests and Computation of Type Curves for Estimating Transmissivity and Storativity*.

Hanna Instruments. (n.d.). *Multiparameter Meter*.

Harb, L., & Roussel, P. (1987). *Ville de Beauvais (Oise) "Plaine du Canada" Etude des conséquences de l'ouverture d'une nouvelle graviére sur l'utilisation des eaux souterraines*.

Healy, R. W., & Cook, P. G. (2002). Using groundwater levels to estimate recharge. *Hydrogeology Journal*, *10*(1), 91–109. https://doi.org/10.1007/s10040-001-0178-0

Healy, R. W., & Scanlon, B. R. (2010). *Estimating Groundwater Recharge*.

Heppner, C. S., & Nimmo, J. R. (2005). *A Computer Program for Predicting Recharge with a Master Recession Curve*.

Ii, C. W. R., & Niemann, W. L. (2001). *Wellskins and slug tests : where ' s the bias ? 243*, 120–132.

Ireson, A. M., Wheater, H. S., Butler, A. P., Mathias, S. A., Finch, J., & Cooper, J. D. (2006). Hydrological processes in the Chalk unsaturated zone - Insights from an intensive field monitoring programme. *Journal of Hydrology*, *330*(1–2), 29–43. https://doi.org/10.1016/j.jhydrol.2006.04.021

Knight, R. I. (1999). Phosphates and phosphogenesis in the Gault Clay (Albian) of the Anglo-Paris Basin. *Cretaceous Research*, *20*(5), 507–521. https://doi.org/10.1006/cres.1999.0163

Kruseman, G. P., & de Ridder, N. A. (1990). *Analysis and Evaluation of Pumping Test Data*.

Lallahem, S. (2002). *Structure et modélisation hydrodynamique des eaux souterraines : application à l'aquifère crayeux de la bordure nord du Bassin de Paris (thesis)*. L'UNIVERSITE DES SCIENCES ET TECHNOLOGIES DE LILLE.

Lapworth, D. J., Baran, N., Stuart, M. E., Manamsa, K., & Talbot, J. (2015). Persistent and emerging micro-organic contaminants in Chalk groundwater of England and France. *Environmental Pollution*, *203*, 214–225. https://doi.org/10.1016/j.envpol.2015.02.030

Lutz, P., & Zouhri, L. (2015). A multidisciplinary hydrogeophysical approach applied to the chalk aquifer using MRS (North of France). *Near Surface Geoscience*.

Mitchell, L., Nimmo, J., & Horowitz, C. (2014). *The Episodic Master Recession (EMR) Program for R*. *1*, 1–9.

Nimmo, J. R., Horowitz, C., & Mitchell, L. (2015). Discrete-storm water-table fluctuation method to estimate episodic recharge. *Groundwater*, *53*(2), 282–292. https://doi.org/10.1111/gwat.12177

Nimmo, J. R., & Perkins, K. S. (2018). Episodic Master Recession Evaluation of Groundwater and Streamflow Hydrographs for Water-Resource Estimation. *Vadose Zone Journal*, *17*(1), 180050. https://doi.org/10.2136/vzj2018.03.0050

Ola, S. A., Fadugba, O. G., & Uduebor, M. A. (2016). Slug Tests for Determination of Hydraulic Conductivity of Contaminated Wells. *Environment and Natural Resources Research*, *6*(2), 156. https://doi.org/10.5539/enrr.v6n2p156

Rumbaugh, D. B., & Rumbaugh, J. O. (2020). *User Manual: Groundwater Vistas Version 8*.

Schlumberger Water Services. (2014). *SLB Diver Manual*.

Tirat, M., Belkessa, R., & avec la colloboration de Fromager, J. P. (1969). Données Géologiques et hydrıgéologiques acquises à la date du 31-12-67 sur le territoire de la feuille topographique au 1/50 000 BEAUVAIS (n° 102) (Oise). *BRGM*.

Todd, D. K., & Mays, L. W. (2004). *Groundwater Hydrology (Third Edition)*.

VanEssen Instruments. (2021). *CTD-Diver*. https://www.vanessen.com/products/data-loggers/ctd-diver/

Yang, L., Qi, Y., Zheng, C., Andrews, C. B., Yue, S., Lin, S., Li, Y., Wang, C., Xu, Y., & Li, H. (2018). A modified water-table fluctuation method to characterize regional groundwater discharge. *Water (Switzerland)*, *10*(4), 1–16. https://doi.org/10.3390/w10040503

Yeh, H., & Chen, Y. (2007). *Determination of skin and aquifer parameters for a slug test with wellbore-skin effect*. 283–294. https://doi.org/10.1016/j.jhydrol.2007.05.029

Zghibi, A., Chenini, I., Zouhri, L., Merzougui, A., & Tarhouni, J. (2015). Modelling of Tracer Movement with Avection-Dispersion Scheme at the LaSalle Beauvais Experimental Site, Beauvais, France. *Journal of Hydrogeology & Hydrologic Engineering*, *04*(03). https://doi.org/10.4172/2325-9647.1000126

Zghibi, A., Zouhri, L., Chenini, I., Merzougui, A., & Tarhouni, J. (2016). Modelling of the groundwater flow and of tracer movement in the porous and fissured media: Chalk Aquifer (Northern part of Paris Basin, France). *Hydrological Processes*, *30*(12), 1916–1928. https://doi.org/10.1002/hyp.10746

Zlotnik, V. A., & McGuire, V. L. (1997). *Multi-level slug tests in highly permeable formations : 2. hydraulic conductivity identification, method verification and field applications*. *204*.

Zouhri, L., & Armand, R. (2019). Groundwater vulnerability assessment of the chalk aquifer in the northern part of France. *Geocarto International*, *0*(0), 1–24. https://doi.org/10.1080/10106049.2019.1637465

Zouhri, L., & Lutz, P. (2010). A comparison of peak and plate electrodes in electrical resistivity tomography: Application to the chalky groundwater of the Beauvais aquifer (northern part of the Paris basin, France). *Hydrological Processes*, *24*(21), 3040–3052. https://doi.org/10.1002/hyp.7719

Zouhri, L., & Lutz, P. (2016). Hydrogeophysical characterization of the porous and fractured media (chalk aquifer in the Beauvais, France). *Environmental Earth Sciences*, *75*(4), 1–15. https://doi.org/10.1007/s12665-015-5209-6

Zouhri, L., Smaoui, H., Carlier, E., & Ouahsine, A. (2009). Modelling of hydrodispersive processes in the fissured media by flux limiters schemes (Chalk aquifer, France). *Mathematical and Computer Modelling*, *50*(3–4), 516–525. https://doi.org/10.1016/j.mcm.2009.04.008

APPENDIX A

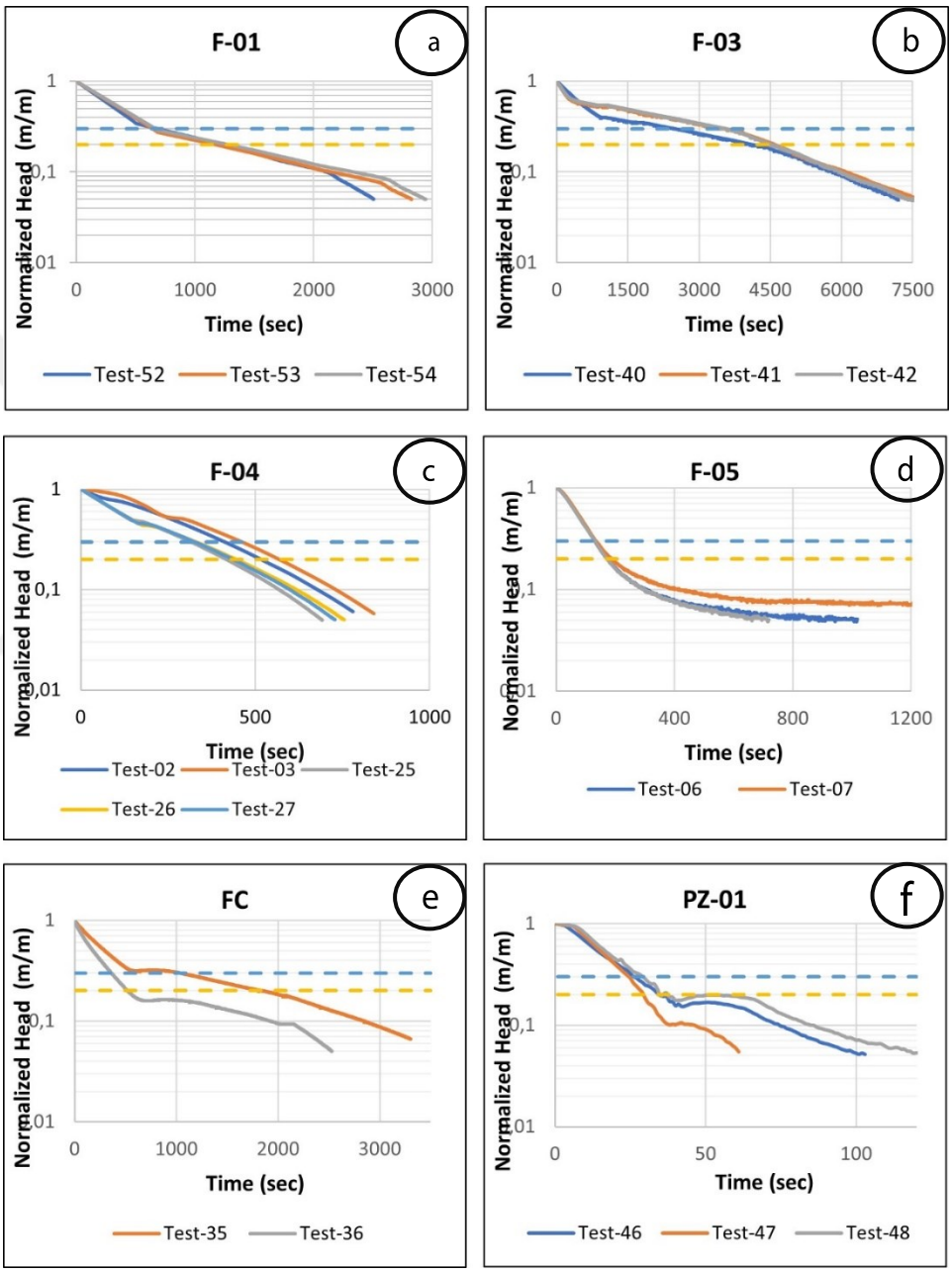

Figure A. 1. Slug test responses on a) F-01 b) F-03 c) F-04 d) F-05 e) FC f) PZ-01

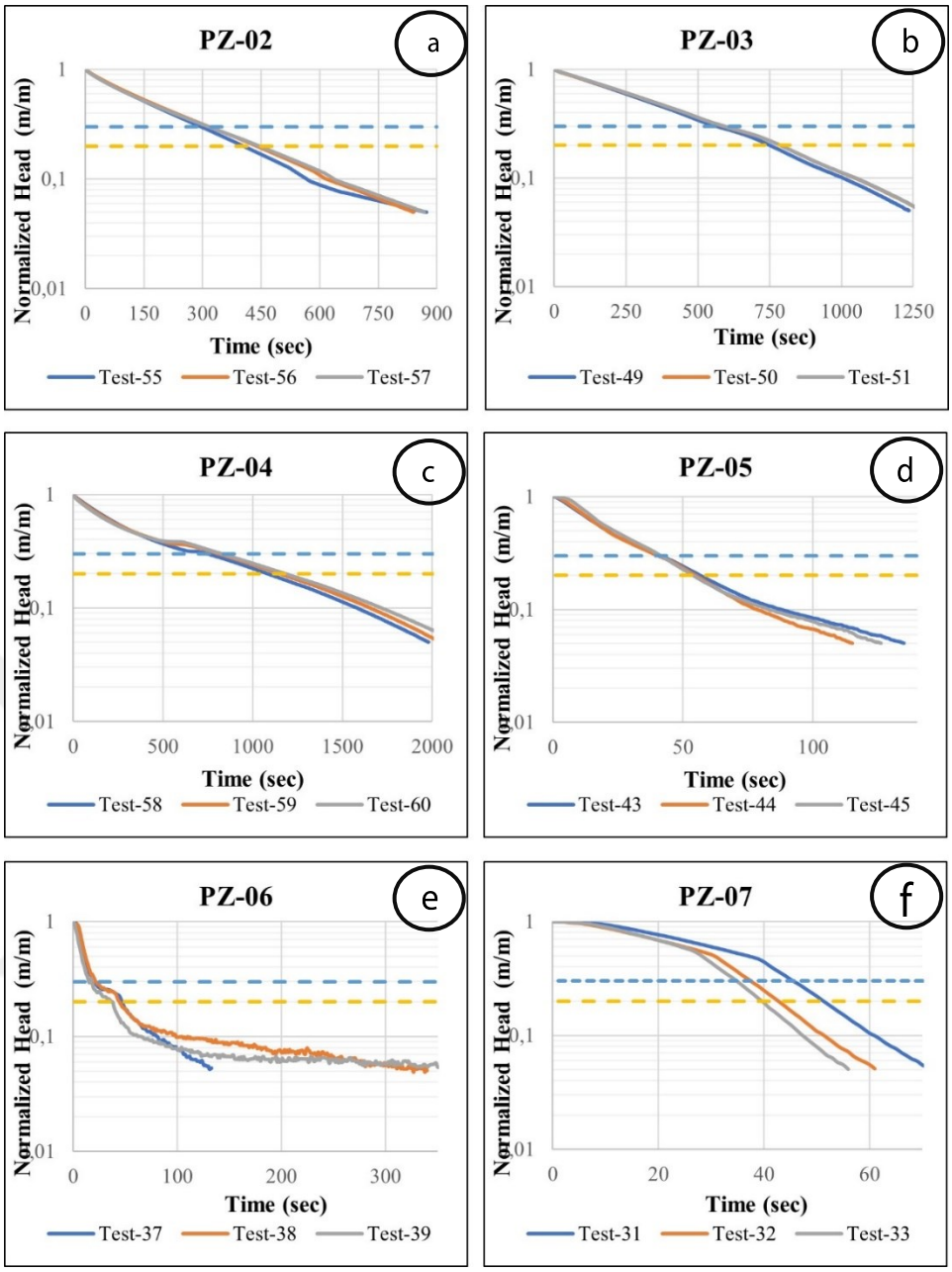

Figure A. 2. Slug test responses on a) PZ-02 b) PZ-03 c) PZ-04 d) PZ-05 e) PZ-06 f) PZ-07

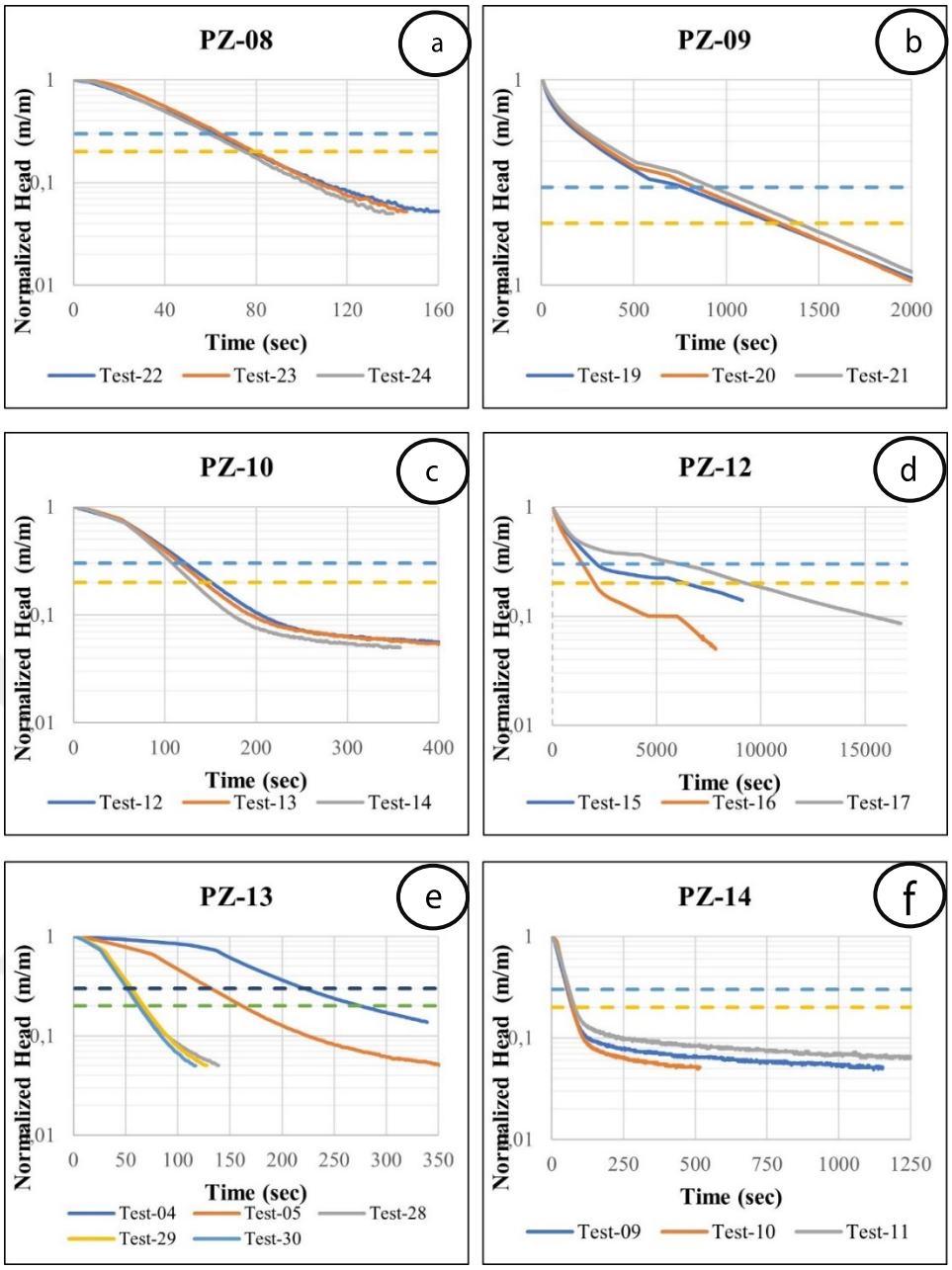

Figure A. 3. Slug test responses on a) PZ-08 b) PZ-09 c) PZ-10 d) PZ-12 e) PZ-13 f) PZ-14

CURRICULUM VITAE

C***n O****N

E-mail : c**********@gmail.com

Education

2020 – 2021 M.Sc. in Hydrogeology and Transfers, University of Poitiers, Poitiers (France)

2019 – 2021 M.Sc. in Department of Geological Engineering, Mugla Sitki Kocman University, Mugla (Turkey)

2007 – 2012 B.Sc. in Department of Geological Engineering, Hacettepe University, Ankara (Turkey)

Professional Experience

February 2021 – September 2021 – Intern, Institut Polytechnique UniLaSalle Beauvais

August 2016 – May 2019 – Geological engineer, UBM Consultancy Services

August 2013 – March 2016 – Field geologist, Yuksel Project International

May 2013 - August 2013 – Field geologist, Geoset Geotechnical Consultancy